CHEMICAL REVIEWS

pubs.acs.org/CR

Review

Amyloid-type Protein Aggregation and Prion-like Properties of Amyloids

Dieter Willbold,* Birgit Strodel, Gunnar F. Schröder, Wolfgang Hoyer, and Henrike Heise

Cite This: *Chem. Rev.* 2021, 121, 8285−8307

Read Online

ACCESS | Metrics & More | Article Recommendations

ABSTRACT: This review will focus on the process of amyloid-type protein aggregation. Amyloid fibrils are an important hallmark of protein misfolding diseases and therefore have been investigated for decades. Only recently, however, atomic or near-atomic resolution structures have been elucidated from various in vitro and ex vivo obtained fibrils. In parallel, the process of fibril formation has been studied in vitro under highly artificial but comparatively reproducible conditions. The review starts with a summary of what is known and speculated from artificial in vitro amyloid-type protein aggregation experiments. A partially hypothetic fibril selection model will be described that may be suitable to explain why amyloid fibrils look the way they do, in particular, why at least all so far reported high resolution cryo-electron microscopy obtained fibril structures are in register, parallel, cross-β-sheet fibrils that mostly consist of two protofilaments twisted around each other. An intrinsic feature of the model is the prion-like nature of all amyloid assemblies. Transferring the model from the in vitro point of view to the in vivo situation is not straightforward, highly hypothetic, and leaves many open questions that need to be addressed in the future.

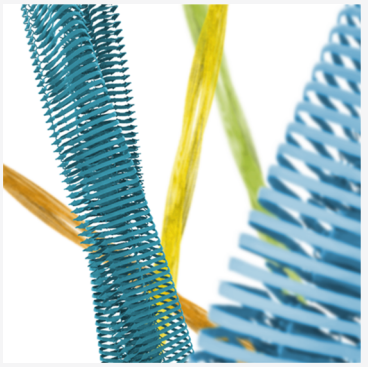

CONTENTS

1. INTRODUCTION

Amyloids have been known and described for more than 100 years, and the history of their identification has been described in earlier reviews.[1,2] Amyloid fibrils are elongated assemblies of identical or almost identical protein or peptide building blocks stacked upon each other within protofilaments that are intertwining each other aligned in a 2-fold helical symmetry. Amyloids have always attracted a lot of interest because they have notoriously been connected to systemic and neurodegenerative diseases. Therefore, the conformation of the protein building blocks within amyloids has been regarded as the *pathogenic* conformation in contrast to their *native* or *physiological* conformations. The *native* conformations of the respective proteins often are intrinsically disordered, but also examples of globularly *well* folded proteins are known. Because amyloids are thermodynamically extremely stable, much more stable than the native conformations of the building blocks, amyloids disprove the general view that natively folded proteins adopt their most stable conformation in their cellular or tissue environment. Obviously, however, there is a very high kinetic barrier for the formation of amyloids, which can be overcome under extremely nonphysiological in vitro conditions, but rarely also under physiological conditions then leading to the respective *protein misfolding* diseases.

Received: March 9, 2021
Published: June 17, 2021

https://doi.org/10.1021/acs.chemrev.1c00196
Chem. Rev. 2021, 121, 8285−8307

There have been many attempts to obtain high-resolution structural information about amyloid fibrils. Transmission electron microscopy (TEM) studies have revealed their long elongated overall structure with mostly helical appearance.[3] From these studies, it was already known that each single fibril had a well-defined appearance over its complete length, e.g., its thickness or the length between protofilament crossovers. Even within a single (in vitro) fibril preparation, however, differences have been observed between the fibrils of the preparation. This is called fibril polymorphism and is one of the remarkable features of amyloids that will be addressed in this review. Solid-state nuclear magnetic resonance (ssNMR) studies gave early insight into supramolecular arrangement of β-strands and secondary structural and some atomic resolution information. However, exact structural information about staggering of β-strands along the fibril axis as well as on handedness could not be obtained unambiguously in these model structures (see section 3.1).

Only, the resolution revolution in the cryogenic electron microscopy (cryo-EM) field[4] allowed us to obtain the first atomic or near-atomic resolution structures starting from 2017 on.[5,6] Since then, many high resolution structures have been published (see section 3.2).

As already mentioned above, this review is not meant to be a descriptive summary of all the beautiful details of all available fibril structures. Instead, this review aims to reconstruct and describe the process of amyloid-type protein aggregation based, wherever possible, on published data and knowledge. Those steps that are not yet well understood will be bridged by old or new hypotheses that will in the best case be amenable to falsification or verification by future experimental work.

2. DEFINITIONS AND NOMENCLATURE

Protein aggregation is a phenomenon observed for practically all protein species under a broad variety of mostly artificial conditions. Starting from a nicely solved solution of, for example, a recombinant protein, changing the solution conditions, e.g., pH, salt concentration or organic cosolvents, easily leads to aggregation of the respective protein. This happens also during large-scale production of recombinant proteins like therapeutically active antibodies and most effort in recombinant protein expression is invested in avoiding aggregation as much as possible. Also, recombinant overexpression of proteins in bacterial cells often leads to so-called inclusion bodies that contain the protein of interest in an mostly undefined insoluble conformation. This all can be summarized as protein aggregation, but this is not the topic of this review.

Sometimes, *protein aggregation* is also used for describing the physiologic assembly of proteins into large homo- or heterogeneous protein assemblies. This is also not the topic of this review, except for those cases where the assemblies are amyloid fibrils such as yeast prions or other functional amyloids.

We will focus on the *amyloid-type protein aggregation* and will call it *amyloid formation* throughout the rest of the manuscript.

Amyloid fibrils are characterized by a repeating substructure that consists of β-strands running perpendicular to the fibril axis, forming cross-β sheets that run parallel along the fibril axis. They have a helical *symmetry* defined by a twist and rise per repeating unit. *Amyloids* usually have a rather slow twist of only a few degrees per subunit. The majority of amyloid fibrils known today consists of two *protofilaments*, which are in most cases symmetric. For the symmetry between the protofilaments, two different arrangements are observed: (1) the C_2 symmetry, where two corresponding layers in the opposing filaments are exactly on the same height along the fibril axis, and (2) an approximate 2_1-screw symmetry, where the layer in one protofilament is in between layers of the opposing protofilament.

Polymorphism refers to the existence of different fibril folds formed by the same amino acid sequence. The different folds ("*morphs*") can differ in the segments of the polypeptide chain that form β-strands or the arrangement of the β-strands in the protofilament, both leading to a different protofilament conformation. In addition, the morphs can differ in the relative arrangement of protofilaments to each other.

Plaques are deposits of many, many *fibrils* that become visible in the light microscope.

The word *oligomer* is often used to denominate small, soluble, and freely diffusible protein assemblies that are not shaped like fibrils but are more globular. Some oligomers have been investigated structurally, yielding high β-sheet content and heterogeneous structures. But much more information has not been obtained so far.

Oligomers are sometimes divided into "*on pathway*" and "*off pathway*" *oligomers*, depending on their ability to further grow into *fibrils*.

The word *protofibril* is often used to denominate elongated protein assemblies that are shorter, more curvy, and disordered than mature fibrils and usually refers to off-pathway assemblies, which are not able to grow into mature fibrils (Figure 1).

The word *prion* has been coined by Stanley Prusiner[7] for amyloid fibrils consisting of prion protein (PrP) in a β-sheet dominated conformation (PrP^{Sc}) that are able to grow and replicate by recruiting monomeric cellular PrP (PrP^{C}) into the

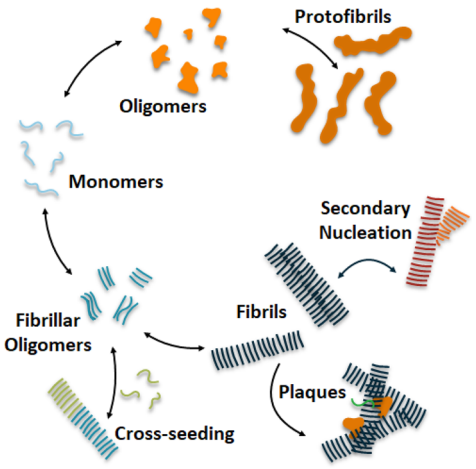

Figure 1. Amyloidogenic proteins aggregate via multiple pathways into different assembly structures. Protein building blocks ("monomers") can form growth-competent fibrillary oligomers that can grow into mature fibrils recruiting more and more identical building blocks. Cross-seeding allows recruitment of nonidentical building blocks. Secondary nucleation has been described as fibril-induced fibril formation. Most oligomers are off-pathway and cannot grow into fibrils but have been described to agglomerate into curvilinear protofibrils. We note that cross-seeding studies often do not reveal whether cross-seeding is in fact due to heterotypic fibril elongation as shown in this figure, or a consequence of heterotypic secondary nucleation.

https://doi.org/10.1021/acs.chemrev.1c00196
Chem. Rev. 2021, 121, 8285−8307

fibril while converting the PrP^{C} conformation into the PrP^{Sc} conformation. It is important to state clearly: the prion protein as such, especially in its PrP^{C} conformation, is not a prion. PrP^{Sc} assemblies are prions, each one of them.

3. STRUCTURAL INFORMATION ON AMYLOIDS

Because there are very beautiful and informative reviews[2,8] on most of the structural details, we summarize here only some details that are relevant for the subsequent thoughts on the process of amyloid formation.

To better understand the information in the following tables, we will first have a look at an example of an in vitro obtained fibril consisting of Aβ(1−42) to explain some relevant properties.[6] A negative stain electron micrograph (Figure 2A) shows an example of a fibril consisting of two protofilaments that intertwine each other (Figure 2B). The negative stain yields a strong contrast of the fibril relative to the background but does not allow high-resolution reconstructions. Ultrafast frozen samples of the same fibril preparation (Figure 2C), but without negative stain, yield only low contrast but allow reconstruction of a density map (Figure 2D) based on many pictures from many fibrils. The density map then allows the calculation of an atomic model of the fibril (Figure 2E).

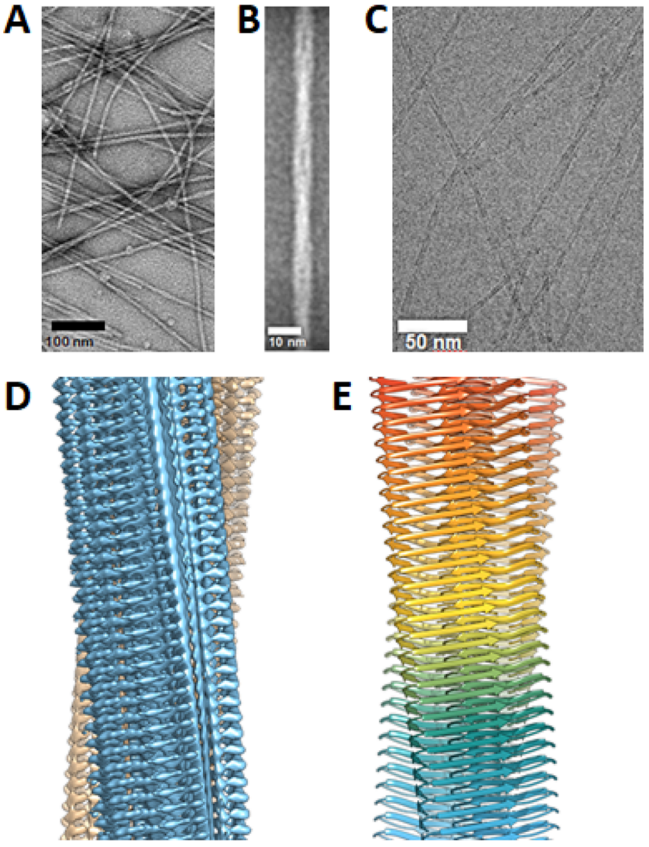

Figure 2. Aβ(1−42) fibrils studied by electron microscopy.[6] (A) Negative-stain electron microscopy imaging shows long ordered amyloid fibrils with high contrast, which show a clear twist when averaged over many fibrils (B). (C) Fibrils embedded in a thin vitrified ice layer imaged by cryo-EM. (D) The reconstructed density map (D) and the corresponding atomic model (in cartoon representation) (E) show the typical cross-β pattern. Reproduced with permission from ref 6. Copyright 2017 AAAS.

Some typical feature of amyloids can be seen in Figure 2E. The protofilaments are composed of many identical Aβ(1−42) protein building blocks that adopted a high proportion of β-strand conformation (Figure 3A). These β-strands do not form intramolecular β-sheets as would be typical for β-sheets within globular proteins but form exclusively intermolecular β-sheets that extend along the complete fibril (Figure 3B,C). This is called "cross-β-sheet" structure. Also, the cross-β-sheet in this example is completely parallel aligned without any sequence register shift. Thus, the example shown here is an amyloid fibril consisting of two protofilaments intertwining each other in a left-handed helix with the building block proteins in a parallel, in register, cross-β-sheet structure.

3.1. Low Resolution Structural Information

As amyloid fibrils are insoluble and noncrystalline, they are not accessible to high-resolution structure determination by X-ray crystallography and solution NMR-spectroscopy. Therefore, until 2017, structural information on amyloid fibrils and protein aggregates was obtained mainly by solid-state NMR spectroscopy and low-resolution electron microscopy (EM) and atomic force microscopy (AFM). In addition, structural information for the interdigitation of amino acid residue side chains of the β-strands within the building blocks was obtained from X-ray crystallographic methods applied to crystals obtained for short segments of amyloidogenic proteins.[9] Initial solid-state NMR characterization involved site-selective isotope labeling combined with accurate distance measurements to yield mainly information about supramolecular arrangement of β-strands within the sheets. A summary of low-resolution structural information on selected amyloid fibrils of short peptide fragments of Aβ as well as a summary of structural models of amyloid fibrils obtained by high-resolution solid-state NMR spectroscopy is given in Table 1.

For a detailed overview of solid-state NMR-studies of amyloid fibrils, we refer to recent review articles.[42−48]

Figure 4 shows possible supramolecular arrangements of β-strands and β-sheets as well as structural motifs. While the ability to form a cross-β-structure may be intrinsic to all proteins regardless of their primary structure,[49] the exact arrangement as well as the supramolecular organization of β-strands and β-sheets seems to depend critically on the amino acid sequence (see Table 1) as well as on the fibrillization conditions. Peptides rich in apolar residues with low amphiphilicity or peptides where antiparallel arrangement can lead to a stacking of charged amino acids of opposite charges have been reported to form antiparallel β-sheets (Figure 4a).[19,38,50] Also, for polyglutamine fibrils (as occurring for example in Huntington's disease), an antiparallel arrangement of β-strands was suggested.[51,52] In nonuniform polar amyloidogenic proteins, on the other hand, hydrogen bonds between asparagine residues and glutamine residues have been described to favor parallel in-register arrangements (Figure 4b,c) in contrast to an out-of-register parallel alignment sketched in Figure 4d, as "polar zippers" can only be formed between amino acid side chains of the same length but not between alternating asparagine and glutamine residues.[53,54] Likewise, in highly amphiphilic peptides, where hydrophobic stacking and formation of hydrogen bonds stabilize interactions between equal residues, the formation of parallel, in-register β-sheets has been suggested to be energetically favored.

https://doi.org/10.1021/acs.chemrev.1c00196
Chem. Rev. 2021, 121, 8285−8307

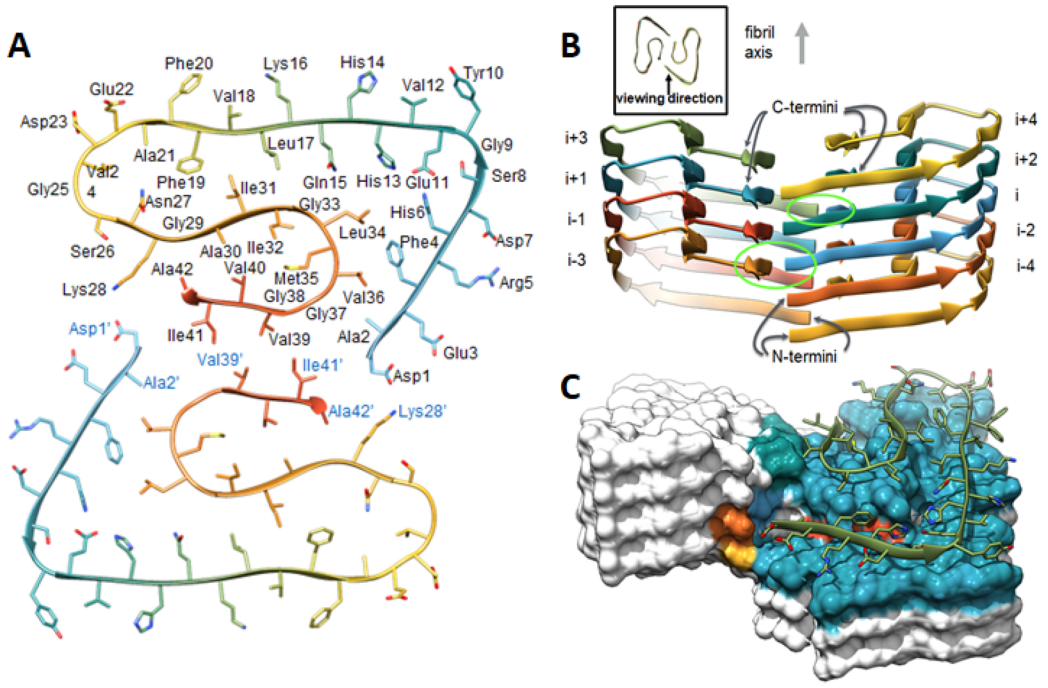

Figure 3. Details of the atomic structure of Aβ(1−42) fibrils.[6] (A) The cross section view of the fibril shows two symmetric protofilaments with an LS-shape. (B) The side view of the atomic model reveals the staggering arrangement of the subunit along the fibril *z*-axis, which results in distinct fibril ends (C). Reproduced with permission from ref 6. Copyright 2017 AAAS.

For most amyloid fibrils from proteins or peptides with more than 20 residues, parallel in-register alignment of β-strands is the preferred alignment (see Tables 1 and 2). The arrangement of individual β-sheets, the cross-β packing, depends not only on the protein but also on the fibrillization conditions and, for in vivo assembled fibrils, possibly also on cofactors. While early studies suggested either a parallel β-sandwich where two parallel in-register β-sheets are connected by a 180° turn (Figure 4e−g) or, for larger proteins, a superpleated β-sheet (Figure 4h), or triangular helical arrangements (Figure 4i),[55] recent high-resolution studies revealed more elaborate folds, like a Greek key motif[27] or an LS-shape,[6] and often two protofilaments are tightly intertwined within the fibril. Recent cryo-EM studies with atomic resolution revealed that the cross-β-section is not necessarily planar in a plane perpendicular to the fibril axis (Figure 4f) but often have a helical shift along the axis (Figure 4g).

Another structural motif, often described for functional amyloids, is the β-solenoid or parallel β-helix, where one protein chain may contribute to more than one layer of β-sheets (Figure 4j).[56] As a consequence, the β-sheets of this example have been suggested to be composed of alternating parallel β-strands from different pseudorepeats of the protein, and β-sheets may in such a case be stabilized not only by polar zippers and hydrophobic contacts but also by electrostatic interactions between amino acid residues with opposite charges in different strands. Prominent examples for such a naturally occurring β-solenoid structures are the prion form of HET-s, a protein from the filamentous fungus *Podospora anserina*,[57−59] and related homologues HELLP[60] and HELLF.[21] Further, this motif has also been suggested (although not confirmed by high-resolution structure determination) for curli in bacterial biofilms[61,62] and yeast prions as Sup35p,[63] although for the latter also a superpleated β-sheet arrangement with a core region depending on the fibrillization temperature was postulated.[64,65] Likewise, low-resolution EM diffraction data of brain derived mammalian prion protein suggest a four-rung β-helical arrangement;[66,67] however, a recent high-resolution cryo-EM structure of a brain-derived mammalian prion clearly revealed a parallel in-register β-sheet arrangement, with only one protofilament in the fibril.[68] Functional amyloids may also be formed by cofibrillization of different proteins with homologous amyloidogenic sequences. A recent example for such a heterodimeric amyloid structure has been suggested for the RIPK1−RIPK3 core of a signaling complex formed in the course of necroptosis.[22] Another possible structural motif deviating from parallel in-register alignment would be an antiparallel β-sheet formed by β-hairpins with alternating β-strands in the sheets (Figure 4k).[28,52]

3.2. High Resolution Structures

Elucidation of atomic resolution structures of amyloid fibrils had to wait for the resolution revolution in the cryo-electron microscopy field.[2,5,6] Most of the so far reported high-resolution fibril structures (summarized in Table 2) were nicely described and discussed already in an excellent recent review.[8] Therefore, in the following, we briefly summarize only the more recent structures that have not been available yet at the time of the previous review.

An ex vivo obtained Aβ fibril structure, most likely consisting of Aβ(1−40),[69] yielded an Aβ(1−40) morph distinct from previous models of Aβ(1−40). The fibril shows a rare right-handed twist, and the interface comprises residues 15−34. A very recent Aβ(1−40) fibril structure amplified from AD brain tissue[70] shows another morph, which is similar in overall shape and has the same residues in the core but is different in sequence register in the protofilament interface. Most prominent is the fact that mass-per-length (MPL) measurements suggest three protein chains per fibril layer, which leads

https://doi.org/10.1021/acs.chemrev.1c00196
Chem. Rev. 2021, 121, 8285−8307

Table 1. Information on the Supramolecular Arrangement of Peptides within the Amyloid Fibril for Different Fragments of Aβ as Determined by ssNMR and List of Amyloid Fibril Structures Deposited in the Protein Data Bank (PDB) Determined by Solid-State NMR Spectroscopy

PDB	publication year	protein	residues	no PF	registry	(first) authors	ref
		(a) Supramolecular Arrangement of Peptides in Fibrils from Aβ Fragments					
na	1995	Aβ(34−42)	9	nd	antiparallel	Lansbury et al.	10
na	1998	Aβ(10−35)	26	nd	parallel in register	Benzinger et al.	11
na	2000	Aβ(16−22)	7	nd	antiparallel	Balbach et al.	12
na	2000	Aβ(1−40)	40	nd	parallel in register	Antzutkin et al.	13
na	2002	Aβ(1−42)	42	nd	parallel in register	Antzutkin et al.	14
na	2004	Aβ(11−25)	15	nd	antiparallel, pH dependent	Petkova et al.	15
na	2007	Aβ(14−23)	10	nd	antiparallel	Bu et al.	16
		(b) Fibril Structures with PDB Entry					
6TUB	2020	β-endorphin		1	parallel in register	Seuring et al.	17
6TI6	2020	Aβ(1−40)		2	parallel in register	Cerofolini et al.	18
6TI5	2020	Aβ(1−40)		2	parallel in register	Cerofolini et al.	18
6TI7	2020	Aβ(1−40)		2	parallel in register	Cerofolini et al.	18
6NZN	2019	glucagon		2	antiparallel	Gelenter et al.	19
6OC9	2019	Aβ_p8S		2	parallel in register	Hu et al.	20
6EKA	2018	HELLF		1	β-helix	Daskalov et al.	21
5 V7Z	2018	RIPK1/RIPK3		2	parallel in register, but heteromolecular	Mompeán et al.	22
5UGK	2017	zinc-binding catalytic peptide		2	parallel in register	Lee et al.	23
5W3N	2017	FUS		1	parallel in register	Murray et al.	24
5KK3	2016	Aβ(M0−42)		2	parallel in register	Colvin et al.	25
2NAO	2016	Aβ(1−42)		2	parallel in register	Wälti et al.	26
2N0A	2016	α-synuclein		1	parallel in register	Tuttle et al.	27
2N1E	2015	hydrogel forming peptide 20 residues		2	antiparallel hairpin	Nagy-Smith et al.	28
2MXU	2015	Aβ(1−42)		1	parallel in register	Xiao et al.	29
2MPZ	2015	AβD23N (Iowa)		3	parallel in register	Sgourakis et al.	30
2MVX	2014	Aβ(1−40) E22Δ (Osaka)		2	parallel in register	Schütz et al.	31
2M4J	2013	Aβ(1−40) brain-seeded		3	parallel in register	Lu et al.	32
5M5M	2013	TTR(105−115)		3*2	parallel in register	Fitzpatrick et al.	33
5M5K	2013	TTR(105−115)		2*2	parallel in register	Fitzpatrick et al.	33
5M5N	2013	TTR(105−115)		1 (2 sheets, peptides)	parallel in register	Fitzpatrick et al.	33
3ZPK	2013	TTR(105−115)		4*2	parallel in register	Fitzpatrick et al.	33
2LNQ	2012	Aβ(1−40) D23N		1	antiparallel	Qiang et al.	34
2LBU	2011	HET-s + Congo red		1	parallel in register	Schütz et al.	35
2KJ3	2010	HET-s		1	β-helix	Van Melckebeke et al.	36
2LMQ	2008	Aβ(1−40)		3	parallel in register	Paravastu et al.	37
2LMP	2008	Aβ(1−40)		3	parallel in register	Paravastu et al.	37
2LMO	2008	Aβ(1−40)		2	parallel in register	Paravastu et al.	37
2LMN	2008	Aβ(1−40)		2	parallel in register	Paravastu et al.	37
2KIB	2008	IAPP(20−29)		2	antiparallel	Madine et al.	38
2E8D	2007	β2m fragment		1	parallel in register	Iwata et al.	39
2NNT	2006	peptide WW domain		1	parallel in register	Ferguson et al.	40
1RVS	2004	TTR(105−115)		1	not defined	Jaroniec et al.	41

to the interpretation that an antiparallel β-hairpin is attached to the surface of the regular cross-2-protofilament fibril.

Two fibril structures of the prion protein (PrP) have been published, one from full-length human PrP(23−231)[71] and one from the fragment PrP(94−178),[72] which comprises a hydrophobic core, known to be fibrillogenic and infectious. Interestingly, the fibril core found from the full-length PrP comprises a different region (residues 170−229) than the fibril core of PrP(94−178) (residues 107−145). Only very recently, a third fibril structure of PrP has been prepublished that reports the structure of full-length PrP fibrils extracted from hamster brains.[68] These fibrils have been shown to be highly infectious, something which has not been demonstrated for the two previously published PrP fibrils.

Two wild-type IAPP fibril conformations (morphs) have been determined; one contains two protofilaments forming a pronounced double-S shape,[73,74] the other[75] shows a very different, rather parallel alignment of the chains along the protofilament interface comprising residues 17−36. Furthermore, the structure of the S20G variant, which is associated with early onset diabetes type-2 has been determined.[73] The structure of this variant is completely different from the known wild-type morphs. Interestingly, two morphs of the S20G variant have been found, one with two symmetric U-shaped

https://doi.org/10.1021/acs.chemrev.1c00196
Chem. Rev. 2021, 121, 8285−8307

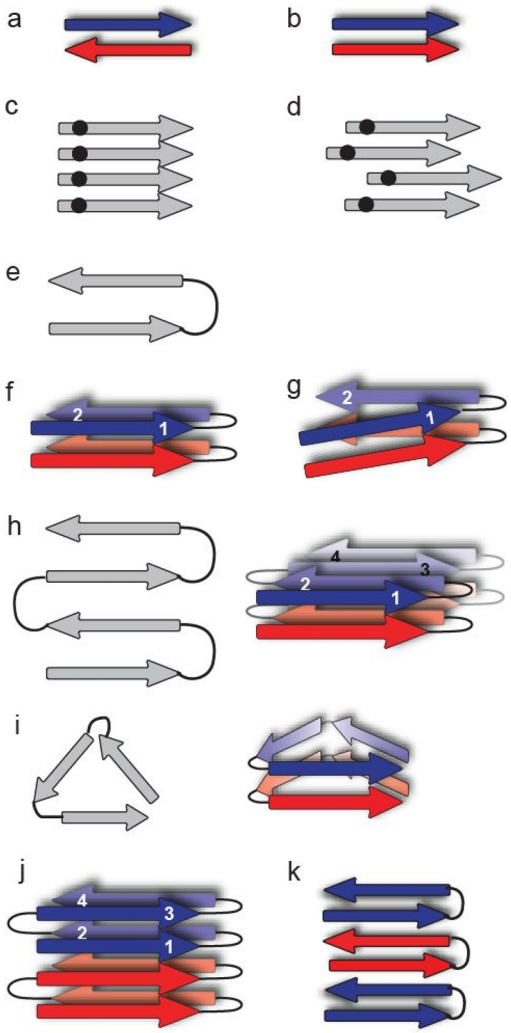

Figure 4. Different arrangements of β-strands and β-sheets and different structural motifs of amyloids: (a) antiparallel, (b) parallel, (c) parallel in register, (d) parallel out-of-register arrangements of β-strands within the sheets. (e–g) Parallel β-sandwich: (e) view along the fibril axis, (f,g) side views with a flat cross-β-section (f) and with (g) a register shift along the fibril axis. (h) Superpleated β-sheet, top and side view, (i) triangular arrangement of β-sheets, top and side view, (j) β-solenoid where one monomer is part of two layers, and (k) antiparallel β-sheet formed by antiparallel β-hairpins. Please note that the shown β-sheet arrangements represent only general common features of possible amyloid folds and are not meant to give a complete overview over all folds observed experimentally so far. Concerning potential β-sheet arrangements, see also the constantly updated collection of information on amyloid structures and models available (https://people.mbi.ucla.edu/sawaya/amyloidatlas).

protofilaments, and a second showing a similar double-U-shape with an additional third filament attached to a secondary site on the surface of one of the U-shaped filaments. This secondary interface suggests a potential role for surface-templated fibril assembly.

Ex vivo structures of α-synuclein from the brain of multiple system atrophy (MSA) patients have been determined[76] and exhibit three new asymmetric morphs. While the single protofilament fold is very similar to the structure of the H50Q variant,[77] the protofilament interface is distinct from all known α-synuclein interfaces and clearly encloses a yet unknown small molecule. Notably, amplification of fibrils from the same brain material by protein misfolding cyclic amplification (PMCA) does not reproduce the same ex vivo polymorphs.[78] Instead several polymorphs were observed which are almost identical to previously determined in vitro structures and only partially resemble the ex vivo fold.

A number of tau fibril structures have been determined in the past, but the relationship between the structure and well-known post-translational modifications (PTMs) of tau remained unclear. Recently, PTMs could be mapped directly onto tau structures.[79] It was found how different PTMs affect the cross-seeding abilities and thus influence tau filament structure, contributing to the structural diversity of tauopathy strains.

Orb2 is the first functional amyloid fibril extracted from its endogenous source (*Drosophila*), of which a structure was determined.[80] Orb2 is associated with memory formation, consolidation, and recall. The fibril shows a hairpin-shaped protofilament structure with an unusal C_3 symmetry, i.e., there are three identical subunits per cross-β layer in the fibril. Moreover, unlike the typical hydrophobic core of pathogenic amyloids, Orb2 exhibits a hydrophilic core consisting almost exclusively of glutamine and histidine residues.

3.3. Polymorphism

As the amyloid conformation is usually not the functional conformation of a protein, but a generic structural motif, which can be adopted by almost all proteins irrespective of the sequence under appropriate conditions, it is not surprising that proteins of identical sequences can form different types of amyloid fibrils. Mesoscopic differences in fibril morphology like differences in fibril width and shape as well as the frequency of helical twists are readily detected by negative stain electron microscopy or AFM. Differences on the molecular level on the other hand are reliably observed by solid-state NMR spectroscopy, where different fibril conformations give rise to different chemical shifts and thus to different spectral fingerprints.[104] Early solid-state NMR-studies on Aβ(1–40) peptides showed that two different isoforms can be obtained in vitro under different fibrillization conditions, and structural details of one fibril form can be transferred to the next fibril generation by seeding.[105] Low-resolution cryo-EM studies of fibrils from Aβ(1–40)[106,107] confirmed the heterogeneous and polymorphic character of Aβ(1–40) amyloid fibrils. Seeded fibril growth with brain extracts from Alzheimer's disease patients yielded different structures of Aβ fibrils with respect to fibrils grown in vitro, and seeding with brain extracts from different patients with distinct clinical subtypes resulted in fibrils with different morphologies.[32,70,108]

Also for α-synuclein, at least five different fibril conformations with differences on the molecular level as well as in the overall fibril morphology and also different sizes of the core region were obtained by fibrillization in vitro and characterized by solid-state NMR spectroscopy.[27,109,110] Cryo-EM studies on in vitro generated α-synuclein fibrils with different C- and N-terminally modifications[90,101–103] as well as ex vivo fibrils from patients with MSA and dementia with Lewy bodies (DLB)[76] confirm the polymorphic nature of α-synuclein fibrils.

In most cases, molecular-level polymorphism correlates with fibril appearance. However, different fibril morphology is not necessarily associated with molecular-level polymorphism. The 32-residue peptide β-endorphin is able to form fibrils with different mesoscopic appearance in vitro. Depending on the presence or absence of salt in the fibrillization buffer, twisted or

https://doi.org/10.1021/acs.chemrev.1c00196
Chem. Rev. 2021, 121, 8285–8307

Table 2. List of All Near-Atomic Resolution Amyloid Fibril Cryo-EM Structures[a]

PDB ID	Res (Å)	Publication Year	Protein	Hand	No PF	Disease	Source	co-factor	Sym	Zipper z-alignment	Δz (Å)	<tilt> (º)	(first) Authors	Reference
7NCK	3.2	2021	alpha-syn	left	1	MSA	ampl	–	asym	staggered	4.9	7.0	Lovestam et al.	78
7NCJ	4.2	2021	alpha-syn	left	2	MSA	ampl	–	asym	staggered	5.2	10.7	Lovestam et al.	78
7NCI	3.5	2021	alpha-syn	left	2	MSA	ampl	–	C2	staggered	5.4	13.9	Lovestam et al.	78
7NCH	3.8	2021	alpha-syn	left	2	MSA	ampl	–	C2	staggered	6.0	14.0	Lovestam et al.	78
7NCG	3.4	2021	alpha-syn	left	2	MSA	ampl	–	C2	staggered	0.1	7.1	Lovestam et al.	78
7NCA	3.5	2021	alpha-syn	left	2	MSA	ampl	–	C2	staggered	0.1	8.8	Lovestam et al.	78
6W0O	2.8	2021	Aβ40	left	3	AD	ampl	–	21	staggered	4.9	8.7	Ghosh et al.	70
7BX7	2.8	2020	hnRNPA1 LC	left	2		in vitro	–	21	staggered	7.7	12.7	Sun et al.	81
6XFM	2.6	2020	FUS LC	left	2		in vitro	–	21	staggered	7.4	11.6	Lee et al.	82
6ZRF	3.6	2020	IAPP	left	2		in vitro	–	21	staggered	5.8	9.8	Gallardo et al.	73
6ZRQ	3.9	2020	IAPP	left	2		in vitro	–	21	staggered	1.7	7.7	Gallardo et al.	73
6ZRR	4.0	2020	IAPP	left	3		in vitro	–	asym	–	2.9	8.8	Gallardo et al.	73
6WQK	3.1	2020	hnRNPA2 LC	left	1		in vitro	–	asym	–	8.7	13.8	Lu et al.	83
6L1T	3.2	2020	alpha-syn	left	2		in vitro	–	21	staggered	13.3	8.9	Zhao et al.	84
6L1U	3.4	2020	alpha-syn	left	3		in vitro	–	asym	staggered	13.0	9.1	Zhao et al.	84
6LNI	2.7	2020	PrP	left	2		in vitro	–	21	staggered	9.7	8.7	Wang et al.	71
6VW2	3.4	2020	IAPP	left	2		in vitro	–	21	staggered	3.4	10.7	Cao et al.	75
6UUR	3.5	2020	PrP(94-178)	left	2		in vitro	–	21	staggered	5.4	11.4	Glynn et al.	72
6LRQ	3.5	2020	alpha-syn	left	2		in vitro	–	21	staggered	6.6	11.4	Sun et al.	85
6VPS	2.6	2020	Orb2	left	3	functional	ex vivo	–	C3	staggered	6.1	6.9	Hervas et al.	80
6Y1A	4.2	2020	IAPP	right	2		in vitro	–	21	staggered	6.0	9.6	Röder et al.	74
6VHA	4.3	2020	tau	left	1	CBD	ex vivo	yes	asym	–	6.9	7.5	Arakhamia et al.	79
6VH7	3.8	2020	tau	left	2	CBD	ex vivo	yes	C2	level	6.9	7.5	Arakhamia et al.	79
6VHL	3.3	2020	tau	left	2	CBD	ex vivo	yes	21	staggered	10.4	9.3	Arakhamia et al.	79
6UFR	2.5	2020	alpha-syn	left	2		in vitro	–	21	staggered	7.9	7.5	Boyer et al.	86
6XYP	3.3	2020	alpha-syn	left	2	MSA	ex vivo	yes	asym	staggered	7.7	8.5	Schweighauser et al.	76
6XYO	2.6	2020	alpha-syn	left	2	MSA	ex vivo	yes	asym	staggered	9.6	9.0	Schweighauser et al.	76
6XYQ	3.1	2020	alpha-syn	left	2	MSA	ex vivo	yes	asym	staggered	7.6	8.5	Schweighauser et al.	76
6TJX	3.0	2020	tau	left	2	CBD	ex vivo	yes	C2	level	6.5	8.5	Zhang et al.	87
6TJO	3.2	2020	tau	left	1	CBD	ex vivo	yes	asym	–	9.4	8.1	Zhang et al.	87
6SST	3.4	2019	alpha-syn	left	2		in vitro	–	21	staggered	9.4	8.0	Guerrero-Ferreira et al.	88
6SSX	3.0	2019	alpha-syn	left	2		in vitro	–	21	staggered	8.4	7.9	Guerrero-Ferreira et al.	88
6PES	3.6	2019	alpha-syn	left	2		in vitro	–	21	staggered	5.8	8.5	Boyer et al.	77
6PEO	3.3	2019	alpha-syn	left	1		in vitro	–	asym	–	4.7	8.0	Boyer et al.	77
6SDZ	3.0	2019	transthyretin	left	1	ATTR	ex vivo	yes	asym	–	6.4	9.7	Schmidt et al.	89
6SHS	4.4	2019	Aβ40	right	2	AD	ex vivo	no	21	staggered	6.3	9.8	Kollmer et al.	69
6OSJ	2.8	2019	alpha-syn	left	2		in vitro	–	21	staggered	4.6	7.9	Ni et al.	90
6OSM	3.4	2019	alpha-syn	left	2		in vitro	–	21	staggered	3.9	9.5	Ni et al.	90
6OSL	3.0	2019	alpha-syn	left	2		in vitro	–	21	staggered	5.4	8.9	Ni et al.	90
6R4R	3.4	2019	SH3	left	2		in vitro	–	21	staggered	15.8	8.1	Röder et al.	91
6N37	3.8	2019	TDP-43	left	2		in vitro	–	21	staggered	9.2	11.1	Cao et al.	92
6N3C	3.3	2019	TDP-43	left	4		in vitro	–	21	staggered	6.4	11.5	Cao et al.	92
6N3B	3.8	2019	TDP-43	left	2		in vitro	–	asym	staggered	10.4	12.5	Cao et al.	92
6N3A	3.3	2019	TDP-43	left	2		in vitro	–	C2	level/stagger	3.5	7.4	Cao et al.	92
6RT0	3.1	2019	alpha-syn	left	2		in vitro	–	21	staggered	8.7	8.7	Guerrero-Ferreira et al.	88
6RTB	3.5	2019	alpha-syn	left	2		in vitro	–	21	staggered	7.0	8.5	Guerrero-Ferreira et al.	88
6IC3	3.3	2019	lambda 1 LC	right	1	AL	ex vivo	–	asym	–	8.1	9.2	Radamaker et al.	93
6NWQ	3.4	2019	tau	left	2	CTE	ex vivo	yes	21	staggered	10.9	9.6	Falcon et al.	94
6NWP	2.3	2019	tau	left	2	CTE	ex vivo	yes	21	staggered	7.1	7.2	Falcon et al.	94
6HUD	4.0	2019	Ig LC	left	1	AL	ex vivo	no	asym	–	9.3	9.8	Swuec et al.	95
6MST	2.7	2019	serum amyloid	right	2	AA	ex vivo	no	21	staggered	9.1	10.7	Liberta et al.	96
6DSO	3.0	2019	serum amyloid	left	2	AA	ex vivo	no	21	staggered	12.9	9.5	Liberta et al.	96
6QJM	3.3	2019	tau	left	1		in vitro	–	asym	–	13.8	13.9	Zhang et al.	97
6QJH	3.3	2019	tau	left	1		in vitro	–	asym	–	24.6	11.9	Zhang et al.	97
6QJP	3.5	2019	tau	left	1		in vitro	–	asym	–	12.9	10.6	Zhang et al.	97
6QJQ	3.7	2019	tau	left	2		in vitro	–	asym	staggered	10.3	9.3	Zhang et al.	97
6GK3	4.0	2018	β2	left	2		in vitro	–	C2	level	5.8	9.0	Iadanza et al.	98
6HRE	3.2	2018	tau	left	2	AD	ex vivo	yes	21	staggered	13.7	10.8	Falcon et al.	99
6HRF	3.3	2018	tau	left	2	AD	ex vivo	yes	asym	staggered	10.8	8.7	Falcon et al.	99
6GX5	3.2	2018	tau	left	1	Pick	ex vivo	no	asym	–	14.8	7.9	Falcon et al.	100
6CU8	3.6	2018	alpha-syn	left	2		in vitro	–	21	staggered	9.0	9.5	Li et al.	101
6CU7	3.5	2018	alpha-syn	left	2		in vitro	–	21	staggered	5.9	9.2	Li et al.	101
6H6B	3.4	2018	alpha-syn	left	2		in vitro	–	21	staggered	5.3	8.0	Guerrero-Ferreira et al.	102
6A6B	3.1	2018	alpha-syn	left	2		in vitro	–	21	staggered	4.5	8.7	Li et al.	103
6FLT	3.4	2018	alpha-syn	right	2		in vitro	–	21	staggered	6.5	11.0	Guerrero-Ferreira et al.	102
5OQV	4.0	2017	Aβ42	left	2		in vitro	–	21	staggered	12.8	10.5	Gremer et al.	6
5O3T	3.4	2017	tau	left	2	AD	ex vivo	yes	asym	staggered	10.6	8.7	Fitzpatrick et al.	5
5O3L	3.4	2017	tau	left	2	AD	ex vivo	yes	21	staggered	12.6	11.3	Fitzpatrick et al.	5
5O3O	3.5	2017	tau	left	2	AD	ex vivo	yes	21	staggered	12.7	11.2	Fitzpatrick et al.	5

[a]Ex vivo structures are highlighted in green. "no PF" denotes the number of protofilaments within a fibril. Δz is the maximum extent of a single chain along the fibril axis. "⟨tilt⟩" is the average absolute angle between the backbone and the plane perpendicular to the fibril axis. Please note: all cross-beta structures are parallel and in register. Therefore, no columns are shown for this information.

https://doi.org/10.1021/acs.chemrev.1c00196
Chem. Rev. 2021, 121, 8285−8307

straight fibrils are obtained. However, the solid-state NMR spectra of both fibril types are identical, suggesting that the molecular conformation of the monomer is the same in both fibril types.[111] Similarly, combined solid-state NMR and cryo-EM studies of in vitro generated fibrils from β2 microglobulin,[98] an 11-residue peptide from transthyretin,[33] and a 12-residue peptide from an immunoglobulin light chain[112] revealed for each of them a similar molecular fold but different fibril morphologies due to different lateral association or different numbers of protofilaments within the fibrils. Also, for tau fibrils from Alzheimer's disease patients, two fibril types, straight and paired helical filaments, were observed. Both fibril types consist of two protofilaments with the same molecular fold but with different lateral association.[5] For tau fibrils derived from brains affected by other tauopathies, however, fibrils with different monomer conformations were observed, suggesting that different disease strains correlate with different fibril polymorphs.[87,94,99]

On the other hand, morphologically homogeneous fibrils may consist of more than one molecular conformer in the fibril unit: amyloid fibrils from the polar peptide fragment GNNQQNY, a fragment from the N-terminus of the yeast prion Sup35p, are composed of three different conformers which give rise to three sets of resonances in solid-state NMR spectra.[113] Likewise, two sets of resonances corresponding to different conformations have been observed for fibrils formed from different constructs of polyglutamines by three different research groups.[51,114,115] Although these different molecular conformations are located in different domains, they still are close in space and occur within the same fibril.

For Aβ(1−40), one fibril type consisting of an asymmetric dimer with two inequivalent conformers within the asymmetric unit has been reported.[116] In peptide fibrils with antiparallel β-sheets, a symmetry break induced by lateral association of β-sheets may give rise to inequivalent monomers within one fibril, as observed in a 10-residue peptide fragment of amylin (IAPP)[50] and for glucagon fibrils.[19]

Thus, a morphologically homogeneous appearance of amyloid fibrils is neither a prerequisite nor sufficient for the existence of a unique single molecular conformation within the fibril.

4. UNDERSTANDING AMYLOID FORMATION IN VITRO

4.1. Thermodynamics and Kinetics of Amyloid Aggregation in Vitro

Amyloid formation requires the presence of the respective building block protein molecules. Those will have a certain conformation, dependent on their preparation and the solution conditions. This defines the starting point of the amyloid formation reaction. For a reliable and reproducible amyloid formation reaction, it is decisive to take utmost care to exclude preformed aggregates, such as for example oligomers, because they may massively influence the reaction in an unforeseeable manner. Depending on the protein of interest (β-amyloid, α-synuclein, tau, SOD1, prion protein, immunoglobulins, transthyretin, etc.), protocols have been developed to take care of this separately and specifically for each of them.

Another important factor for amyloid formation reactions is the concentration of the building block protein molecules. Several-fold higher concentrations are needed than what is usually known as their physiological concentrations. Just as an example, several μM Aβ are usually used for aggregation experiments, although the physiological concentration is sub-nM. That means more than thousand-fold higher concentrations are needed than what is present in the brain in order to observe fibril formation in vitro within hours. In analogy to crystallization setups, this highly artificial in vitro condition has been named supersaturation.[117] Nonetheless, some of the proteins mentioned above still need several days of incubation and sometimes additional support, such as stirring or cofactors, for a successful de novo fibril formation reaction to occur.

This clearly suggests that there is a high kinetic barrier to amyloid formation, most likely because several building blocks need to be built into a "seed" fibril before it has reached a minimal size to become stable enough to populate, and of which some may be able to elongate and grow.

Typically, the fibril formation is observed in a thioflavin T (ThT) fluorescence experiment. ThT is a fluorescent dye that increases its fluorescence intensity when it attaches to regular cross-β fibril structures. The ThT fluorescence therefore correlates with the amount (mass) of amyloid fibrils in the sample. The roughly sigmoidal ThT increase with incubation time can be separated into three phases, the so-called lag phase, the exponential growth phase, and the saturation plateau phase (Figure 5). During the last phase, the building blocks become

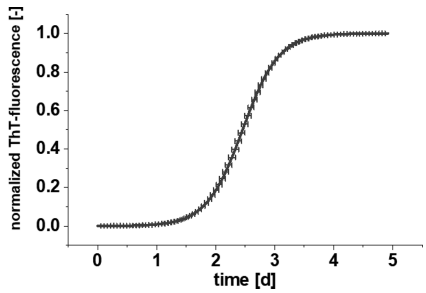

Figure 5. Example of a ThT fibril formation experiment. Shown is the time-dependent ThT fluorescence intensity for the example of α-synuclein. The lag phase in this example is about 1 day. The lag phase is followed by a steep increase in ThT positive assembly formation and a saturation plateau closer toward the end when the monomer building blocks become more and more depleted, thereby limiting further fibril growth.

less and less concentrated and so the amyloid formation slows down while the remaining building block concentration becomes too low for further amyloid growth.

Although also other methods have been used to follow fibril formation, e.g., light scattering, CD spectroscopy, and even neutron scattering,[118,119] the ThT assay seems to be the most popular one, due to its practicality and sufficient sensitivity at protein concentrations applied in in vitro assays.

Primary nucleation is obviously the first and essential reaction to start amyloid formation. Its apparently high reaction order and high activation energy, however, make it a very rare event during all phases of the ThT experiment. Thus, already during the lag phase, all other reactions are relevant for the quantitative interpretation of the experiment. Soon after the first primary nucleation events, elongation, fragmentation, and surface-catalyzed secondary nucleation become increasingly dominating. The rate at which the complete reaction continues can be modeled and predicted using an integrated rate equation based on all potentially relevant reactions: primary nucleation, elongation, fragmenta-

https://doi.org/10.1021/acs.chemrev.1c00196
Chem. Rev. 2021, 121, 8285−8307

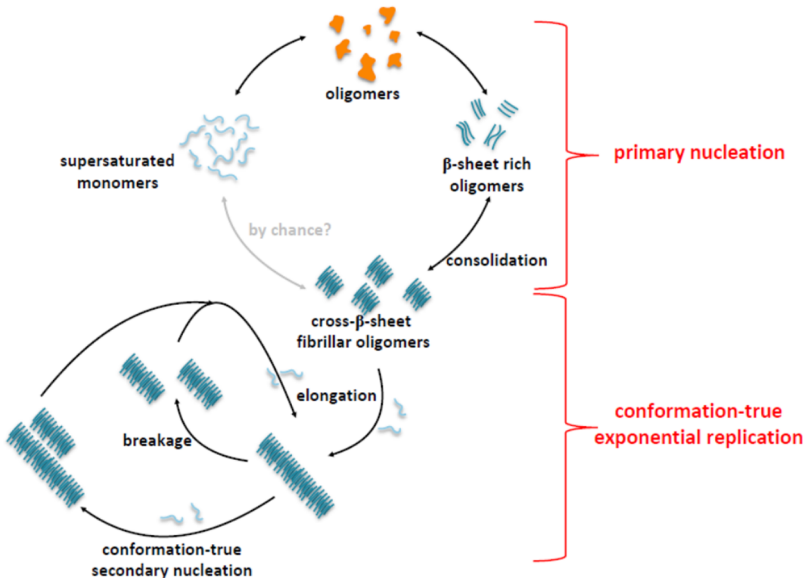

Figure 6. Fibril selection mechanism in vitro. In vitro fibril formation requires high (supersaturated) monomer concentrations. Initial oligomers will have very heterogenic conformations. Soon, the oligomers contain high β-sheet content, but it takes time before substantial fibril growth is observed. Obviously, the β-sheet-rich oligomers are not growth competent yet. Either the consolidation of the oligomers into cross-β-sheeted fibrillary oligomers is a very slow consolidation process, or the formation of the first growth competent fibrillary oligomer seed is an extremely rare event. Only such fibrils that contain all relevant information for their growth and are able to pass this information to "daughter" fibrils after breakage or by conformation-preserving (conformation-true) secondary nucleation will grow and replicate exponentially and thus supersede all nongrowing assemblies but also all growth-competent fibrils that are not able to pass their conformation onto the recruited building blocks.

tion, secondary nucleation, and dissociation.[120−123] The development of the hereby obtained "master equation" is certainly a breakthrough for the quantitative treatment of amyloid formation.

The quantitative description of fibril formation tells us already some important general properties of amyloid formation. First, amyloid formation is thermodynamically favorable. The free energy ΔG for amyloid formation is negative and actually is equal to RTln(cf), where cf is the final concentration of the remaining monomer building blocks after net fibril formation has terminated and the system is in thermodynamic equilibrium. Second, because high concentrations of building block proteins need to be present for amyloid formation to take place in a realistic time frame, amyloid formation is obviously kinetically unfavorable. For the example Aβ, it has been shown that the smallest assemblies that populated during aggregation have the size of at least five or six monomer building blocks.[119] There are many reports on the observation of dimers, trimers, or tetramers, but they solely rely on cross-linking experiments or "semi-denaturing" SDS PAGE analysis. The observation of a cross-link between two monomers, however, cannot rule out that there have been more than the two monomers in the assembly from which the cross-linked dimer originated. And in "semi-denaturing" SDS PAGE analysis, the species that appear as having the molecular weight of a dimer can well have just a different charge/size ratio as a monomer with maximum possible charge/size ratio (in a fully denaturing SDS PAGE), and apparent Aβ dimers, trimers, and tetramers in SDS page were shown to be even SDS induced.[124] Likewise, different SDS-stabilized Aβ oligomers, consisting of 4−16 monomers, were characterized by solution NMR.[125,126] Efforts to study the very early events in nucleation formation have been reported, providing initial insight into the structural diversity of early oligomers.[127]

4.2. Fibril Selection Mechanism in Vitro: Why Do Amyloid Fibrils Look the Way They Do?

Let us (again) start with a typical fibril formation experiment in vitro. We start with artificially high monomer concentrations to avoid the lag phase being months or years. Depending on the protein species, the monomer concentration, presence of surfaces, including phase separations, and the solution conditions, the first oligomeric assemblies form. Most, if not all of them will be "off-pathway" to fibrils. Thus, only a very minor fraction will be ThT positive and have cross-β-sheet structure. The example of Aβ has recently been investigated in this regard. At time points during the lag phase, a high fraction of Aβ is contained already in β-sheet rich oligomers.[128,129] Solid-state NMR confirmed that these oligomers do have a high content of β-sheet structures and are very heterogeneous.[129,130] The high degree of heterogeneity may not be too surprising because we know that even under very similar conditions, fibril polymorphism is observed. Thus, we can assume that also oligomers that form for example during the lag phase will have very heterogenic conformations. Indeed, heterogeneity of monomer building block conformations can especially be assumed within each single oligomer because not all monomer building blocks will experience the same environment. Even if one assumes oligomers to be small fibrils, their ends will make up a substantial fraction of the total monomer building blocks. Although oligomers already contain high β-sheet content, it takes a while before substantial fibril growth is observed. Very obviously, almost all or all of the oligomers are not (yet) competent to grow. Either the consolidation of the oligomers into small fibrils is a very slow process, or the formation of a growth competent fibril seed is a much rarer event than oligomer formation.

The question is what the process of consolidation could be that transforms elongation-incompetent oligomers into small elongation-competent fibrils. The artificially high monomer

https://doi.org/10.1021/acs.chemrev.1c00196
Chem. Rev. 2021, 121, 8285−8307

concentration may be compared to a supercritical concentration of monomers at the edge of a phase conversion or separation. This supersaturation condition[117] can either lead to a macroscopic phase separation or to a microscopic "micelle"-like oligomer formation. If oligomer formation is favored, it may be a relatively unordered process leading to more or less unspecific "micelle"-like clumping of the monomers. This will lead to a very heterogeneous mixture of possibly already β-strand containing building blocks of a somehow homogeneous size, like little droplets. The extremely high local concentration of monomer building blocks within each oligomer might then lower the kinetic barriers for the formation of amyloid-type cross-β sheeted fibril seeds. This could possibly be the consolidation of elongation-incompetent oligomers into small elongation competent cross-β-sheeted fibrils. Whether such a consolidation is needed or whether a few growth competent assemblies have been formed also by chance will be hard to distinguish, but as soon as growth competent assemblies are present, they will grow and consume monomers. The monomer concentration will decrease, and, because all assembly species are in equilibrium with the monomers, the least stable oligomers will be destabilized first and subsequently others, too.

Fibril conformations that induce the conformation of their already recruited building blocks in the "new" monomer building blocks while recruiting them at the fibril ends will grow truly autocatalytically while preserving their three-dimensional conformation ("morph"). Such fibrils, and only such fibrils, will contain all relevant information for their growth and be able to pass this information to "daughter" fibrils after breakage. Such conformation-preserving (conformation-true) autocatalytic growth will supersede all non-growing assemblies but also all growth-competent fibrils that are not able to pass their conformation onto recruited building blocks. Thus, macroscopically, we will find only conformation-true autocatalytic growth competent fibrils, of possibly different ("polymorphic") three-dimensional conformations. All other types will be outcompeted and will not populate. If more than one conformation will be autocatalytically growth competent, polymorphism will emerge among the growth-competent assemblies, which we can certainly call fibrils now. Among the different fibril morphs, those will dominate that grow faster and possibly fragment more frequently. Efficiency in secondary nucleation might also be decisive for the dominating fibril morphs, but only if the secondary nucleation is conformation-true, i.e., if the conformation of the matrix fibril passes its conformation onto the secondary seeds. Otherwise, the conformation of the matrix fibril is lost and it will not populate further. In any case, at the end of the in vitro fibril formation experiment, we will find only fibril morphs that have made it through a tough selection procedure that is reminiscent of the "pre-biotic" evolution of autocatalytic metabolic cycles (Figure 6).[131] The here described fibril selection procedure for parallel in-register cross-β-sheet amyloid structures is not in conflict with frequently reported antiparallel β-sheet rich structures in aggregates that have been obtained by (fast) precipitation instead of a (slow) selection process for amyloid growth.

All the high-resolution fibril structures reported so far (Table 2), no matter whether in vitro- or ex vivo-obtained, must have gone through such a selection process. Thus, it is interesting that all of them report a parallel in register alignment of their monomer building blocks within the protofilaments. So far, there is not a single exception. This suggests that the parallel in register alignment is an intrinsic and essential property of autocatalytically growth competent amyloid fibrils. As already mentioned in section 3.1, one exception may be that one monomer building block can well be expected to contribute more than one β-sheet layer per building block, but this may still be regarded as parallel in register relative to the monomer building blocks. Thus, reports of such structures resolved at high resolution are to be expected possibly in the near future, already. This includes also the β-solenoid fold suggested for the HET-s prion by ssNMR[57] and low-resolution cryo-EM.[59] On the other hand, it is not straightforward to imagine, that antiparallel alignments support conformation-preserving ("conformation-true") elongation. Antiparallel alignments of monomer building blocks do not allow subsequent building blocks to have exactly the same individual conformation within or along the protofilament, rendering conformation-true growth practically impossible. Interestingly and fully in agreement with this, there is a report on antiparallel β-sheets in Aβ42 oligomers that have been characterized as being growth-incompetent.[132]

4.3. Prion-like Properties of Amyloids

Prions are composed of host-encoded protein building blocks that adopt, in contrast to their physiologic conformation, alternative conformations, which are autocatalytically self-perpetuating and self-propagating. As just described in the previous section, amyloid fibril conformations, which populate during growth, are true autocatalytic growth competent fibrils that pass their conformation onto newly recruited building blocks. Therefore, autocatalytic behavior is intrinsic to amyloid folds that macroscopically populate. One may say that this is already the most important property to call them prion-like, because amyloids are able to replicate under consumption of monomer building blocks (Figure 6).

Of course, prion-like properties also include other aspects, for example, transmissibility from one organism to another, with or without the transmissibility of pathology or a disease phenotype in parallel, but this is certainly a matter of efficiency, both of the transmission pathway (oral, through the gastrointestinal tract, or even iatrogenic via growth hormone injections[133]) and of individual or species barriers.

The emerging view on amyloids as being prion or prion-like has helped to make progress in the understanding of the underlying principles for the observed spread of pathology in the brains affected by neurodegenerative diseases.[134−143] Also, the discussion on the role of amyloid conformations as the underlying principle for "strains" and potential disease subtypes has profited from the adaptation of prion principles into the general field of protein misfolding diseases.[144−163] It will also have an impact on the development of new treatment strategies for such diseases.[164−167]

5. AMYLOID FORMATION IN VIVO

Amyloid aggregation in the in vivo environment is even more complex than under controlled in vitro conditions. First, the in vivo concentrations of the various amyloid proteins are often low compared to concentrations applied in in vitro assays, making in these cases the formation of growth-competent assembly (primary nucleation) a really rare event. An example along this line is Aβ, for which concentrations between 10^{-11} and 10^{-9} M have been reported for its physiological presence in cerebrospinal fluid (CSF),[168−171] which is probably close to its concentration in interstitial fluid.[172] The values for α-

https://doi.org/10.1021/acs.chemrev.1c00196
Chem. Rev. 2021, 121, 8285−8307

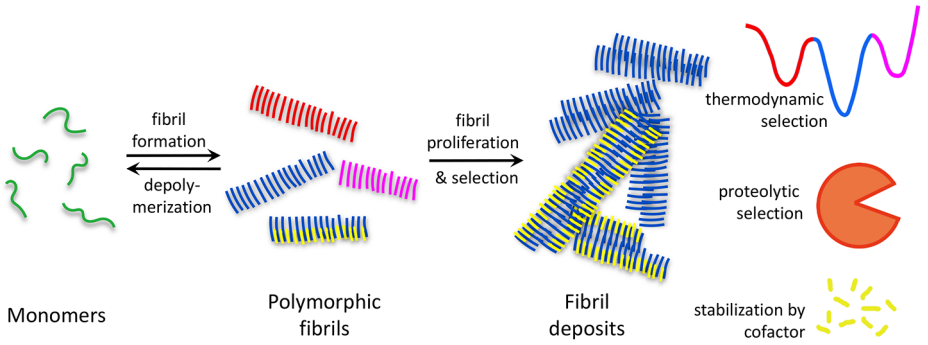

Figure 7. Fibril selection mechanisms in vivo. Initially, different fibril polymorphs may form, of which under in vivo conditions, which are characterized by low concentrations of the amyloid proteins, years for the aggregation to take place, and the presence of a myriad of other molecules, only one fibril structure proliferates. Three different selection mechanisms for the proliferation of fibrils in tissue have been proposed: (i) thermodynamic selection, where only the fibril structure with the highest thermodynamic stability resists depolymerization; (ii) proteolytic selection, where the fibril structure most resistant against proteolytic cleavage survives; (iii) selection by cofactor, where the proliferating fibril structure is stabilized by another, coaggregating molecule.

synuclein and IAPP can be similar: 10^{-10} to 10^{-9} M in the case of α-synuclein in CSF[173,174] and 10^{-12} to 10^{-10} M for IAPP in plasma.[175−177] On the other hand, the average intracellular α-synuclein concentration in the brain is 35−70 μM,[178,179] while the concentration of IAPP in the secretory granules of the beta cells is 1−10 mM.[180] Thus, amyloid proteins can occur at very different concentrations in vivo, and it is surprising that some of them endure so long without aggregating, which suggests that there must be aggregation inhibitory cofactors around, while others like Aβ undergo aggregation at all.

The concentration of Aβ in brain fluids is well below the apparent critical fibril concentration, i.e., the concentration of monomers when fibrils start forming in vitro within a reasonable time span, which is in the low micromolar range.[181,182] However, the formation of Aβ oligomers occurs already below this critical fibril concentration.[181−186] For this, a lower limit of about 90 nM has been determined as the critical aggregation concentration of monomers which is required for Aβ to undergo any kind of aggregation in vitro.[187] Thus, one may either claim that the physiological Aβ concentration can indeed reach the apparent critical aggregation concentration for oligomer formation under certain conditions or in certain compartments. Alternatively, Aβ monomer concentrations well below the apparent critical aggregation concentration may lead to oligomer or fibril formation, albeit at an extremely low rate. Considering that age is the single greatest risk factor for Alzheimer's disease, the low concentration of Aβ may be outweighed given the abundance of time that could allow Aβ aggregation to occur even though it is a very rare event. Familial mutations that increase the concentration of aggregation prone Aβ species will slightly increase the rate of primary nucleation, making this a bit less rare and therefore happening usually earlier in life, on average. The most radical mutation in this regard is certainly trisomy 21 with an increase of Aβ concentration by 50%. Environmental conditions, e.g., infections[188−190] or traumatic brain injuries,[191,192] may have a similar effect. Moreover, it seems that due to age, the local concentration of Aβ can be increased, too. An analysis of the age dependence of the kinetics of Aβ in the brain revealed a dramatic slowing of amyloid-β turnover with increasing age: a 2.5-fold increase in Aβ half-life from 3.8 to 9.4 h over five decades.[193] The age associated Aβ slowing of turnover rate may be a general effect of all brain proteins, similar to the general slowing of body and muscle protein turnover rates by ∼30−40% (1.4−1.7 fold decrease in rate) with increasing age.[194,195] Although, given that for Aβ the slow-down is 2.5-fold, it may also be specific to Aβ. It was further estimated how long Aβ would need to accumulate to reach amounts of amyloidosis typical of AD. The conclusion was that plaques build up over about 40 years, which is above the estimate of 15−20 years that was made earlier.[196] Independent of whether this number is 20 or 40 years, it shows that fibril formation in vivo is a slow or rare process, which most likely results from the interplay of long times enabling this rare event to happen and local increases in Aβ concentration in the aging brain.

The slow aggregation in vivo plays a role in generally reducing the heterogeneity of fibrils in vivo, as discussed in the previous section. It was suggested that only a few of the different fibril morphologies that a protein can adopt are associated with disease.[197] Moreover, fibrils from patient tissue tend to be structurally different from fibrils of the same precursor protein but grown in vitro. Examples include fibrils formed as a result of systemic amyloid light-chain (AL) amyloidosis,[198,199] Aβ fibrils in Alzheimer's disease,[69] tau fibrils in tauopathies,[97] or αS fibrils that formed during multiple system atrophy.[200] The protein building blocks of ex vivo fibrils often adopt the same conformation. This applies not only to fibrils from different deposition sites within the same patient or animal[198] but even includes fibrils extracted from different humans or animals that suffered from the same disease variant and expressed the same allelic variant of the fibril precursor protein.[69,89,99,198,200,201] On the other hand, variants of the same amyloidosis tend to be related to different morphologies and biochemical characteristics of the fibrils.[94,202,203] These findings suggest that specific fibril morphologies and disease variants are interrelated. This observation raises many questions such as what the relationship between fibril morphology and pathogenicity is.

Another question is why there are fewer and different morphologies in fibrils extracted from diseased tissue than in those formed in vitro. Comparison of the stabilities of ex vivo and in vitro transthyretin (TTR) amyloid fibrils revealed that the energy release during synthetic fibril formation is smaller than for the natural fibrils.[204] This stability assessment was accomplished using the strong chaotropic agent guanidine thiocyanate (Gdn-SCN), which causes the depolymerization of the fibrils by disrupting the hydrogen bonding network in the solvent. This allowed the determination of the free energies of

https://doi.org/10.1021/acs.chemrev.1c00196
Chem. Rev. 2021, 121, 8285−8307

fibril formation, ΔG, which led to the conclusion that the tissue-extracted TTR fibrils have a higher thermodynamic stability than the in vitro TTR obtained fibrils. Because resistance toward depolymerization originates from intermolecular interactions, such as hydrogen bonds in β-sheets, the conjecture is that the structure of the ex vivo obtained TTR fibrils must involve more of such interactions, possibly also more or longer β-sheets.

For the case of serum amyloid A (SAA), it was described in a comparative study of ex vivo and in vitro obtained SAA fibrils that these fibrils differ in their morphologies.[197] The ex vivo obtained fibrils contain nine β-strands involving 39 residues per protein, whereas the in vitro obtained fibrils have only seven β-strands with 27 residues of each of the proteins being involved. Both the ex vivo and in vitro obtained SAA fibrils, however, were found to be relatively unstable in a Gdn-HCl solution. Instead it was suggested that the ex vivo obtained SAA fibrils were considerably more stable against degradation by proteases than the tested in vitro obtained fibrils, which puts forward proteolytic selection as an important property for in vivo fibrillization and this agrees also to findings made for Aβ amyloid fibrils. Also, in this case, the fibrils extracted from patient tissues were more protease-resistant than those formed in vitro.[69,205] The studies conclude that in vivo the fibril morphology with the highest proteolytic resistance, i.e., the one that escapes endogenous clearance mechanisms most efficiently, survives for longer periods of time and can therefore proliferate in a prion-like manner, so that eventually a specific fibril morphology prevails. In summary, the smaller diversity of fibril morphologies observed in vivo is accompanied by a higher thermodynamic stability or higher resistance against proteasomal degradation of the fibrils, which most likely is not only a consequence but probably also the cause of the dominance of a specific fibril morph for a specific disease variant (Figure 7).

The prion-like efficacies of Aβ and tau deposits from human AD patients have been reported to be inversely correlated with the age of the donors.[206] This can be interpreted in a way that the higher the "seeding" and growth potential of a certain fibril conformation is, the earlier in life pathology and disease symptoms are induced. This would suggest that replication speed of amyloids correlates with initiated damage in brain tissue.

The role of liquid−liquid phase separations and liquid to solid phase transitions has been heavily investigated in the recent years,[207−211] but much more insight of their roles in transiently increasing local concentrations of amyloidogenic proteins in cells and their relevance for disease development are needed.

The formation of amyloid fibrils in vivo further differs from the in vitro situation in that many more different molecules are present in vivo. In fact, fibrils extracted from diseased tissue are virtually always associated with nonfibrillar biomolecules, such as apolipoprotein E,[212] collagen,[213] metal ions,[214] glycosaminoglycans (GAGs),[215] and lipids.[216] Initially, these accessory molecules were considered as passive bystanders or contaminants of the amyloid fibrils. Today we know that cofactors can be essential constituents of amyloid fibrils (Figure 7). Examples of ex vivo obtained fibril structures that contain unidentified densities include α-synuclein fibrils resulting from multiple system atrophy[200] and tau fibrils from corticobasal degeneration human brain tissue[79] (Table 2).

To gain an understanding of the influences of the various metal ions and biomolecules on the kinetics of the amyloid aggregation process and the resulting fibril morphologies, hundreds, if not thousands, of biophysical studies were performed. Most of these cofactors influence the amyloidogenic process, with the effects ranging from aggregation enhancement, modulation of the fibril morphology or, in some cases, aggregation retardation.[217] The emerging view is that amyloid formation in vivo does not only result from protein misfolding or age- and/or genetics-related accumulation of aggregation-prone proteins but also may be dependent on the interaction of the amyloidogenic protein precursor with extrinsic factors and/or its (bio)chemical microenvironment to set off the fibrillization process. A prototypical example in this regard is the aggregation of tau, which in vitro is generally triggered with the help of cofactors, most commonly heparin, RNA, or arachidonic acid. A common aspect of these cofactors is the presence of charges, which suggests that they are required for tau aggregation. This was indeed confirmed by a study, which reported that seeding of tau aggregation is not only facilitated by polyanionic cofactors (heparin or RNA in this study) but that both seeded and recombinant mature fibrils depolymerize into monomers when their cofactor was removed.[218] A follow-up study further revealed that these cofactors act as templating reactant that causes tau conformational rearrangements into aggregation-competent species, which is best accomplished by heparin compared to the other possible cofactors.[219] The subsequent aggregation into ThT-active fibrils results from an interplay between tau and the cofactor that form intermediate complexes, which in the case of mild cofactors, such as polyU RNA, require further seeding to overcome the energy barrier for fibril formation. On the basis of these results, an idea was put forward according to which in vivo tau could form metastable, "inert" complexes with cofactors, which only upon encountering a seed undergo irreversible transition to a β-sheet structure.[219]

Another example demonstrating the intimate coupling between protein and cofactor during fibrillization is provided by α-synuclein. In a study that used α-synuclein filament preparations extracted from brains demented by MSA to seed recombinant human α-synuclein in vitro, it was found that the structures of the seeded assemblies were different from those of the seeds.[78] The conclusion therefore was that in vivo additional cofactors must play a role in the propagation of pathology. These cofactors have not been resolved yet, but their identification will be central for resolving the prion-like spreading of α-synuclein amyloids in MSA. This statement of course holds true for all other amyloid diseases, too, where the selection (evolution) of true autocatalytic growth-competent fibrils led to (polymorphic) conformations that include one or more cofactors as part of the fibril.

Here, it may be of relevance to summarize that the spontaneous formation of a true autocatalytic growth-competent fibril seed is probably an extremely rare event. Especially under physiological conditions, which include low monomer concentrations and high abundance of confounding or supporting molecules, the spontaneous formation of such a seed can be expected to be very rare and growth can also be expected to be slow. No matter how slow the growth and replication will be, it has the potential to be exponential, and finally, after decades of individual lifetime, the chance of rare events will have accumulated to almost certainty and

https://doi.org/10.1021/acs.chemrev.1c00196
Chem. Rev. 2021, 121, 8285−8307

exponential replication during subsequent decades of lifetime easily becomes problematic for the affected organ or organism.

Therefore, there must be general and specific defense strategies of organisms that have evolved because amyloid formation and replication is a thread to all living cells and organisms.

6. AMYLOIDS AND EVOLUTION OF DEFENSE STRATEGIES

Because amyloid formation and replication is a thread to all living cells and organisms, evolution must have developed general and specific defense strategies. Indeed, all living organisms have a dedicated arsenal of cellular machineries to achieve an equilibrium between protein formation as well as protein degradation and clearance. This is often summarized as the proteostasis network. The most obvious part of the proteostasis network relevant to combat protein aggregation, are the chaperones that assist proteins in adopting their nonamyloid native and functional conformation.[220−222] Also, degradation of proteins via the proteasome pathway[223,224] or via autophagy[225] is relevant in that regard.[226]

Eukaryotic organisms exhibit an evolutionary highly conserved process for the degradation of cytoplasmic components ranging from bulk degradation to the removal of whole organelles and invading pathogens, which commonly is referred to as autophagy.[227,228] However, with macrophagy, chaperone-mediated autophagy, and microautophagy, at least three different types of autophagy exist,[229] of which macrophagy is the best studied and according to general practice is referred simply to as autophagy hereafter. (Macro)autophagy plays an important role during cell homeostasis including basal, deprived, as well as pathological conditions and is usually induced in response to a variety of physiological and environmental stimuli.[227,228]

Characteristic for the induction of autophagy is the formation of the so-called phagophore, an isolation membrane, which expands progressively to trap diverse cytoplasmic components and ultimately sequesters the cargos into a separate, double-membrane compartment, the autophagosome. The biogenesis of autophagosomes is a highly complex membrane reorganizing process involving more than 40 autophagy-related (ATG) proteins. These ATGs operate in consecutive physiologically continuous but mechanistically distinct steps and are arranged in separate functional clusters. Ultimately, autophagosomes fuse with lysosomes (or the vacuole in yeast) to form autolysosomes, where resident hydrolases degrade the captured material.

In contrast to nonselective autophagy, by which parts of the cytoplasm are randomly engulfed by autophagosomes for bulk degradation and recycling back to the cytoplasm for reuse, selective autophagy is responsible for the clearance of specific components including damaged organelles and invading pathogens.[230] The ATG8 protein, which split in several paralogues in higher organisms (e.g., LC3s and GABARAPs in mammals), is required for phagophore initiation, elongation, and maturation[231] but also plays a critical role during selective autophagy. When carboxy terminally conjugated, the lipid phosphatitylethanolamine anchors ATG8-type proteins among others to autophagosomal membranes.[232] That way these small ubiquitin-like modifiers can act as a docking platform for the selective recruitment of cargos through selective autophagy receptors (SAR) like p62/SQSTM1 (sequestome-1).[233]

Autophagy and the ubiquitin−proteasome system are the two major quality control pathways responsible for cellular homeostasis.[234] Misfolded proteins that cannot be rescued by chaperones and that are inaccessible for the ubiquitin−proteasome system (UPS) end up in protein aggregates. Under certain circumstances such aggregates can undergo degradation by a selective form of autophagy, which is called aggrephagy.[235,236] Flagging the misfolded protein aggregates by ubiquitin seems to be a key event in this process, as ubiquitination triggers aggregate recognition by SARs through their ubiquitin-binding domain (UBA). Because SARs also have at least one ATG8 protein interacting motif (named AIM, LIR, or GIM), they thus mediate aggregate recruitment by bridging the aggregate and the ATG8-type protein, which itself is anchored to the inner membrane of the autophagosome. Recent studies indicate that proteins targeted for aggrephagy are not simple protein aggregates but rather form liquid-like protein condensates and that the related properties of the condensates may be crucial in the initiation of aggrephagy.[237]

Autophagy-dependent degradation has been reported for a multitude of pathological protein aggregates consisting of, e.g., tau, SOD1, α-synuclein, and Huntingtin and more.[238−241] Its failure has been reported to contribute to the progression of neurodegenerative and psychiatric diseases associated with these and other proteins, including AD, Parkinson's disease (PD), amyotrophic lateral sclerosis (ALS), frontotemporal dementia (FTD), Huntington's disease (HD), bipolar disorder, and schizophrenia.[242−245] According to current evidence, there is a possibility that autophagy may be a druggable target and, consequently, its modulation may be a promising therapeutic option for central nervous system (CNS) diseases.[246−249] Furthermore, the autophagic machinery is also involved in unconventional protein secretion and autophagy-dependent secretion, which are also fundamental mechanisms for toxic protein disposal, underlying a crosstalk between the autophagic and the endosomal system. In this regard, part of our knowledge of the secretory functions of autophagy originates from studies dealing with α-synuclein and β-amyloid precursor protein (βAPP), as reviewed recently.[250]

More specifically, it has been suggested that evolution has selected protein amino acid sequences against amyloid formation, at least for the highly abundant protein species.[251] Also, it has been reported that human CSF contains a factor that decelerates secondary nucleation.[252]

For many years, research has concentrated especially to identify factors that influence specifically Aβ formation, aggregation, and clearance. One of the most interesting observations is the identification of the cellular conformation of the pion protein (PrP^C) as a receptor of Aβ oligomers,[253,254] and PrP^C is also able to bind to fibrillar Aβ.[255−257] This capacity of PrP^C extends beyond Aβ: oligomers or sonicated fibrils of α-synuclein and tau interact with the same site in the PrP^C N-terminus as Aβ and also inhibit long-term potentiation.[258−260]. Moreover, the N-terminal domain of PrP^C was shown to interact with β-structure conformers of yeast prion proteins and designed β-peptides.[261] This emphasizes the notion that these different aggregates share a similar structure. Although, it has been suggested that binding of $A\beta_{oligo}$ to membrane-anchored PrP^C mediates Aβ toxicity during AD by mediating neuron and synapse damage[253,262,263] via Fyn-kinase activation,[264,265] this has also been questioned.[266−269] It became very clear that soluble PrP[270] as well as its N-terminal fragment PrP(23−111)[271,272] have a

https://doi.org/10.1021/acs.chemrev.1c00196
Chem. Rev. 2021, 121, 8285−8307

protective role by inhibiting Aβ fibrillization and sequestration of Aβ oligomers. Although being first described as a mediator of cytotoxicity of Aβ oligomers, PrP^C is doing what has been suggested already for potential treatment strategies for Alzheimer's disease (AD), namely to cap the ends of Aβ fibrils to prevent them from further growth.[273] One may speculate even whether this is the long sought physiological function of PrP^C. This is supported by the observation that PrP^C is accumulated in aged human brains even prior to any AD related pathology.[274,275]

Compacting otherwise freely diffusible Aβ aggregates into plaques, rendering them insoluble and in total less toxic, may also be a defense strategy of our brain. Especially microglia have been recognized to be decisively involved in protective activities but also in pro-inflammatory activities even, increasing stress on astrocytes and neurons in neurodegenerative diseases. For example, genome-wide association studies (GWASs) have tried to link the risk of late onset Alzheimer's disease to human genes, and have identified numerous genes that are expressed in microglia: CR1, CD33, TREM2, APOE, MS4a, INPP5D/SHIP1, ABCA7, PLCG2, SPI1, ABI3, BIN1, PICALM, CD2AP, and SORL1. While the roles of each risk factor is not yet well understood and the current stage of investigation is nicely summarized in a recent review,[276] we focus here on two of the most studied protein factors, apolipoprotein E (ApoE) and triggering receptor expressed on myeloid cells 2 (Trem2). Trem2 is expressed in the brain specifically in microglia, and reduction of its function, e.g., by mutations, has been clearly linked to increased risk of Alzheimer's disease.[277] This supports that microglia have evolved functions that are relevant for clearance of extracellular amyloids in the brain. This is further supported by the observation that TREM2 expression correlates positively with age as well as with AD progression and probably serves as a compensatory mechanism in response to amyloids.[278] Trem2 has been shown to directly interact with ApoE, another highly interesting protein.[279] ApoE is not only expressed in brain but also in liver, adipose tissue, and arteries. This could hint at systemic-wide protective mechanisms that have evolved against amyloids. It is well-known that carriers of the ApoE4 allele have a significantly increased risk for AD, whereas the ApoE2 allele reduces the risk compared to the ApoE3 allele. ApoE2 has originally been identified as a longevity gene,[280] further supporting a systemic effect of the ApoE function in aging and neurodegeneration.[281,282] In that regard, future studies should also investigate the role of the liver for the protection against amyloids. The liver, as the main organ responsible for substance clearance and detoxification, can be expected to play an important role here. Indeed, a recent study has shown accumulation of α-synuclein to a higher degree in the liver of Parkinson's disease patients that compared to control subjects.[283]

Many more general and specific protection strategies against toxic and self-replicating amyloid species will be identified in the future and may become new targets for therapeutic strategies to protein misfolding diseases in general.

7. CONCLUSION AND OUTLOOK

Amyloid type protein aggregation is one of the best examples for the role of structural biology in scientific progress within the life sciences. Because X-ray crystallography could not play the role it has played in basically all other aspects of life sciences, and NMR spectroscopy has some limitation for elucidation of long-range structural aspects that are relevant in amyloids, the amyloid field has been suffering from the lack of atomic resolution structures of elongated amyloids. With the advent of the resolution revolution in cryo-electron microscopy the first near-atom resolution structures in 2017 brought not only highly esthetic and beautiful structures of amyloids but also immediate inspiration for, in the static structures of course unobservable, elongation mechanisms.[5,6]

Since then, many more structures have been reported, but many questions remained unanswered: What is the general toxic principle of (disease-relevant) amyloids? Why are some of them toxic, while others, especially some of the systemic amyloids, are just laying around in tissue and while growing displace healthy cells and only therefore cause disease? Is pathology dependent on the conformation of amyloid fibrils? What is the structure of primary nuclei? What exactly is secondary nucleation? How do intracellular amyloids spread between cells? How efficient, if at all, are amyloids transferred from one organism to another? Are PrP prions the only amyloids that are relevant for interindividual passage?

AUTHOR INFORMATION

Corresponding Author

Dieter Willbold − *Institute of Biological Information Processing, Structural Biochemistry, IBI-7, Forschungszentrum Jülich GmbH, 52425 Jülich, Germany; Institut für Physikalische Biologie, Heinrich-Heine-Universität Düsseldorf, 40225 Düsseldorf, Germany; Research Center for Molecular Mechanisms of Aging and Age-Related Diseases, Moscow Institute of Physics and Technology (State University), 141700 Dolgoprudny, Russia;* orcid.org/0000-0002-0065-7366; Email: d.willbold@fz-juelich.de

Authors

Birgit Strodel − *Institute of Biological Information Processing, Structural Biochemistry, IBI-7, Forschungszentrum Jülich GmbH, 52425 Jülich, Germany; Institute of Theoretical and Computational Chemistry, Heinrich-Heine-Universität Düsseldorf, 40225 Düsseldorf, Germany;* orcid.org/0000-0002-8734-7765

Gunnar F. Schröder − *Institute of Biological Information Processing, Structural Biochemistry, IBI-7, Forschungszentrum Jülich GmbH, 52425 Jülich, Germany; Physics Department, Heinrich-Heine-Universität Düsseldorf, 40225 Düsseldorf, Germany*

Wolfgang Hoyer − *Institut für Physikalische Biologie, Heinrich-Heine-Universität Düsseldorf, 40225 Düsseldorf, Germany*

Henrike Heise − *Institute of Biological Information Processing, Structural Biochemistry, IBI-7, Forschungszentrum Jülich GmbH, 52425 Jülich, Germany; Institut für Physikalische Biologie, Heinrich-Heine-Universität Düsseldorf, 40225 Düsseldorf, Germany;* orcid.org/0000-0002-9081-3894

Complete contact information is available at: https://pubs.acs.org/10.1021/acs.chemrev.1c00196

Notes

The authors declare no competing financial interest.

Biographies

Dieter Willbold studied biochemistry in Tübingen (Germany), Bayreuth (Germany), and Boulder (Colorado, USA). He completed

https://doi.org/10.1021/acs.chemrev.1c00196
Chem. Rev. 2021, 121, 8285−8307

his Ph.D. in 1994 at the University of Bayreuth. After some more years in Bayreuth and a couple of research visits, e.g., at the Sackler School of Medicine of the Tel-Aviv University, in 1998, he was leading his independent junior research group at the Institute for Molecular Biotechnology in Jena, Germany. In 2001, Willbold became an associate Professor at the Heinrich-Heine University in Düsseldorf. Since 2004, he is full professor and chair of the Institute of Physical Biology in Düsseldorf and director of the Institute of Biological Information Processing at the Forschungszentrum Jülich. His main interests are protein interactions with physiological and artificial ligands, high resolution structural biology, aging, neurodegeneration, neuropathic pain, and autophagy.

Birgit Strodel studied chemistry at the Heinrich-Heine University Düsseldorf and the University of North Carolina at Chapel Hill (USA) and received her Ph.D. in Theoretical Chemistry from the University of Frankfurt/Main in 2005. She then joined the group of Prof. David J. Wales at Cambridge University (UK) as a postdoctoral research associate. Since 2009, she heads the Computational Biochemistry Group at Forschungszentrum Jülich and was appointed Professor at Heinrich-Heine University Düsseldorf in 2011. Her research interests primarily involve the thermodynamics and kinetics of protein aggregation as well as protein−membrane interactions and drug design.

Gunnar F. Schröder studied physics in Göttingen (Germany) and Caen (France). He performed his Ph.D. work at the Max-Planck-Institute for Biophysical Chemistry (supervised by Helmut Grubmüller) and received his Ph.D. in 2004 from the University of Göttingen. He did a postdoc at Stanford University in the groups of Michael Levitt and Axel Brunger. Since 2009, Schröder is a group leader at the Forschungszentrum Jülich and since 2018 associate professor at the Heinrich-Heine University Düsseldorf (Germany). He works on computational method development and application of cryo-EM with a focus on amyloid structure.

Wolfgang Hoyer is Assistant Professor at the Institute of Physical Biology at Heinrich-Heine University Düsseldorf. He studied chemistry in Münster (Germany), York (UK), and Zürich (Switzerland). He received his Ph.D. in Biochemistry in 2004 at the University of Münster for work performed at the Max Planck Institute for Biophysical Chemistry, Göttingen. He then moved to Gothenburg (Sweden) for a three-year postdoctoral study in the group of Torleif Härd. Since 2009, he is a group leader at Heinrich-Heine University Düsseldorf and at Forschungszentrum Jülich. His main research interests are the mechanism of amyloid assembly, structural motifs in amyloidogenic intrinsically disordered proteins, and inhibition of amyloid formation.

Henrike Heise studied chemistry at the TU München (Germany) and Modena and Florence (Italy). She received her Ph.D. on NMR spectroscopy on paramagnetic solids (supervised by Frank H. Köhler) at the TU München in 1999. From 2000 to 2002 she was a postdoc at the UC Berkeley, California, on NMR methods development in the group of Alex Pines. From 2002 to 2007, she worked as a Liebig fellow of the Fonds of the Chemical Industry at the Max-Planck-Institute for Biophysical Chemistry in Göttingen on biomolecular solid-state NMR-spectroscopy. Since 2007, she is an associate professor at the Heinrich-Heine University in Düsseldorf and Forschungszentrum Jülich. Her main interests are biomolecular solid-state NMR spectroscopy and DNP enhancement.

REFERENCES

(1) Sipe, J. D.; Cohen, A. S. Review: History of the Amyloid Fibril. *J. Struct. Biol.* **2000**, *130*, 88−98.

(2) Iadanza, M. G.; Jackson, M. P.; Hewitt, E. W.; Ranson, N. A.; Radford, S. E. A New Era for Understanding Amyloid Structures and Disease. *Nat. Rev. Mol. Cell Biol.* **2018**, *19*, 755−773.

(3) Sunde, M.; Blake, C. The Structure of Amyloid Fibrils by Electron Microscopy and X-Ray Diffraction. *Adv. Protein Chem.* **1997**, *50*, 123−159.

(4) Callaway, E. The Revolution Will Not Be Crystallized: A New Method Sweeps through Structural Biology. *Nature* **2015**, *525*, 172−174.

(5) Fitzpatrick, A. W. P.; Falcon, B.; He, S.; Murzin, A. G.; Murshudov, G.; Garringer, H. J.; Crowther, R. A.; Ghetti, B.; Goedert, M.; Scheres, S. H. W. Cryo-EM Structures of Tau Filaments from Alzheimer's Disease. *Nature* **2017**, *547*, 185−190.

(6) Gremer, L.; Schölzel, D.; Schenk, C.; Reinartz, E.; Labahn, J.; Ravelli, R. B. G.; Tusche, M.; Lopez-Iglesias, C.; Hoyer, W.; Heise, H.; et al. Fibril Structure of Amyloid-B(1−42) by Cryo-Electron Microscopy. *Science* **2017**, *358*, 116−119.

(7) Prusiner, S. B. Molecular Biology of Prion Diseases. *Science* **1991**, *252*, 1515−1522.

(8) Gallardo, R.; Ranson, N. A.; Radford, S. E. Amyloid Structures: Much More Than Just a Cross-β Fold. *Curr. Opin. Struct. Biol.* **2020**, *60*, 7−16.

(9) Sawaya, M. R.; Sambashivan, S.; Nelson, R.; Ivanova, M. I.; Sievers, S. A.; Apostol, M. I.; Thompson, M. J.; Balbirnie, M.; Wiltzius, J. J.; McFarlane, H. T.; et al. Atomic Structures of Amyloid Cross-Beta Spines Reveal Varied Steric Zippers. *Nature* **2007**, *447*, 453−457.

(10) Lansbury, P. T.; Costa, P. R.; Griffiths, J. M.; Simon, E. J.; Auger, M.; Halverson, K. J.; Kocisko, D. A.; Hendsch, Z. S.; Ashburn, T. T.; Spencer, R. G. S.; et al. Structural Model for the β-Amyloid Fibril Based on Interstrand Alignment of an Antiparallel-Sheet Comprising a C-Terminal Peptide. *Nat. Struct. Mol. Biol.* **1995**, *2*, 990−998.

(11) Benzinger, T. L. S.; Gregory, D. M.; Burkoth, T. S.; Miller-Auer, H.; Lynn, D. G.; Botto, R. E.; Meredith, S. C. Propagating Structure of Alzheimer's β-Amyloid(10−35) Is Parallel β-Sheet with Residues in Exact Register. *Proc. Natl. Acad. Sci. U. S. A.* **1998**, *95*, 13407−13412.

(12) Balbach, J. J.; Ishii, Y.; Antzutkin, O. N.; Leapman, R. D.; Rizzo, N. W.; Dyda, F.; Reed, J.; Tycko, R. Amyloid Fibril Formation by A Beta(16−22), a Seven-Residue Fragment of the Alzheimer's Beta-Amyloid Peptide, and Structural Characterization by Solid State NMR. *Biochemistry* **2000**, *39*, 13748−13759.

(13) Antzutkin, O. N.; Balbach, J. J.; Leapman, R. D.; Rizzo, N. W.; Reed, J.; Tycko, R. Multiple Quantum Solid-State Nmr Indicates a Parallel, Not Antiparallel, Organization of Beta-Sheets in Alzheimer's Beta-Amyloid Fibrils. *Proc. Natl. Acad. Sci. U. S. A.* **2000**, *97*, 13045−13050.

(14) Antzutkin, O. N.; Leapman, R. D.; Balbach, J. J.; Tycko, R. Supramolecular Structural Constraints on Alzheimer's Beta-Amyloid Fibrils from Electron Microscopy and Solid-State Nuclear Magnetic Resonance. *Biochemistry* **2002**, *41*, 15436−15450.

(15) Petkova, A. T.; Buntkowsky, G.; Dyda, F.; Leapman, R. D.; Yau, W. M.; Tycko, R. Solid State Nmr Reveals a Ph-Dependent Antiparallel Beta-Sheet Registry in Fibrils Formed by a Beta-Amyloid Peptide. *J. Mol. Biol.* **2004**, *335*, 247−260.

(16) Bu, Z.; Shi, Y.; Callaway, D. J. E.; Tycko, R. Molecular Alignment within {Beta}-Sheets in A{Beta}14−23 Fibrils: Solid-State NMR Experiments and Theoretical Predictions. *Biophys. J.* **2007**, *92*, 594−602.

(17) Seuring, C.; Verasdonck, J.; Gath, J.; Ghosh, D.; Nespovitaya, N.; Wälti, M. A.; Maji, S. K.; Cadalbert, R.; Güntert, P.; Meier, B. H.; et al. The Three-Dimensional Structure of Human β-Endorphin Amyloid Fibrils. *Nat. Struct. Mol. Biol.* **2020**, *27*, 1178−1184.

(18) Cerofolini, L.; Ravera, E.; Bologna, S.; Wiglenda, T.; Böddrich, A.; Purfürst, B.; Benilova, I.; Korsak, M.; Gallo, G.; Rizzo, D.; et al. Mixing Aβ(1−40) and Aβ(1−42) Peptides Generates Unique Amyloid Fibrils. *Chem. Commun.* **2020**, *56*, 8830−8833.

(19) Gelenter, M. D.; Smith, K. J.; Liao, S.-Y.; Mandala, V. S.; Dregni, A. J.; Lamm, M. S.; Tian, Y.; Xu, W.; Pochan, D. J.; Tucker, T.

https://doi.org/10.1021/acs.chemrev.1c00196
Chem. Rev. 2021, 121, 8285−8307

J.; et al. The Peptide Hormone Glucagon Forms Amyloid Fibrils with Two Coexisting B-Strand Conformations. *Nat. Struct. Mol. Biol.* **2019**, *26*, 592−598.
(20) Hu, Z.-W.; Vugmeyster, L.; Au, D. F.; Ostrovsky, D.; Sun, Y.; Qiang, W. Molecular Structure of an N-Terminal Phosphorylated β-Amyloid Fibril. *Proc. Natl. Acad. Sci. U. S. A.* **2019**, *116*, 11253−11258.
(21) Daskalov, A.; Martinez, D.; Coustou, V.; El Mammeri, N.; Berbon, M.; Andreas, L. B.; Bardiaux, B.; Stanek, J.; Noubhani, A.; Kauffmann, B.; et al. Structural and Molecular Basis of Cross-Seeding Barriers in Amyloids. *Proc. Natl. Acad. Sci. U. S. A.* **2021**, *118*, No. e2014085118.
(22) Mompeán, M.; Li, W.; Li, J.; Laage, S.; Siemer, A. B.; Bozkurt, G.; Wu, H.; McDermott, A. E. The Structure of the Necrosome Ripk1-Ripk3 Core, a Human Hetero-Amyloid Signaling Complex. *Cell* **2018**, *173*, 1244−1253.
(23) Lee, M.; Wang, T.; Makhlynets, O. V.; Wu, Y.; Polizzi, N. F.; Wu, H.; Gosavi, P. M.; Stöhr, J.; Korendovych, I. V.; DeGrado, W. F.; et al. Zinc-Binding Structure of a Catalytic Amyloid from Solid-State Nmr. *Proc. Natl. Acad. Sci. U. S. A.* **2017**, *114*, 6191−6196.
(24) Murray, D. T.; Kato, M.; Lin, Y.; Thurber, K. R.; Hung, I.; McKnight, S. L.; Tycko, R. Structure of Fus Protein Fibrils and Its Relevance to Self-Assembly and Phase Separation of Low-Complexity Domains. *Cell* **2017**, *171*, 615−627.
(25) Colvin, M. T.; Silvers, R.; Ni, Q. Z.; Can, T. V.; Sergeyev, I.; Rosay, M.; Donovan, K. J.; Michael, B.; Wall, J.; Linse, S.; et al. Atomic Resolution Structure of Monomorphic Aβ42 Amyloid Fibrils. *J. Am. Chem. Soc.* **2016**, *138*, 9663−9674.
(26) Wälti, M. A.; Ravotti, F.; Arai, H.; Glabe, C. G.; Wall, J. S.; Böckmann, A.; Güntert, P.; Meier, B. H.; Riek, R. Atomic-Resolution Structure of a Disease-Relevant Aβ(1−42) Amyloid Fibril. *Proc. Natl. Acad. Sci. U. S. A.* **2016**, *113*, E4976−E4984.
(27) Tuttle, M. D.; Comellas, G.; Nieuwkoop, A. J.; Covell, D. J.; Berthold, D. A.; Kloepper, K. D.; Courtney, J. M.; Kim, J. K.; Barclay, A. M.; Kendall, A.; et al. Solid-State NMR Structure of a Pathogenic Fibril of Full-Length Human [Alpha]-Synuclein. *Nat. Struct. Mol. Biol.* **2016**, *23*, 409−415.
(28) Nagy-Smith, K.; Moore, E.; Schneider, J.; Tycko, R. Molecular Structure of Monomorphic Peptide Fibrils within a Kinetically Trapped Hydrogel Network. *Proc. Natl. Acad. Sci. U. S. A.* **2015**, *112*, 9816−9821.
(29) Xiao, Y.; Ma, B.; McElheny, D.; Parthasarathy, S.; Long, F.; Hoshi, M.; Nussinov, R.; Ishii, Y. A[Beta](1−42) Fibril Structure Illuminates Self-Recognition and Replication of Amyloid in Alzheimer's Disease. *Nat. Struct. Mol. Biol.* **2015**, *22*, 499−505.
(30) Sgourakis, N. G.; Yau, W.-M.; Qiang, W. Modeling an in-Register, Parallel "Iowa" Aβ Fibril Structure Using Solid-State Nmr Data from Labeled Samples with Rosetta. *Structure* **2015**, *23*, 216−227.
(31) Schütz, A. K.; Vagt, T.; Huber, M.; Ovchinnikova, O. Y.; Cadalbert, R.; Wall, J.; Güntert, P.; Böckmann, A.; Glockshuber, R.; Meier, B. H. Atomic-Resolution Three-Dimensional Structure of Amyloid B Fibrils Bearing the Osaka Mutation. *Angew. Chem., Int. Ed.* **2015**, *54*, 331−335.
(32) Lu, J.-X.; Qiang, W.; Yau, W.-M.; Schwieters, C. D.; Meredith, S. C.; Tycko, R. Molecular Structure of β-Amyloid Fibrils in Alzheimer's Disease Brain Tissue. *Cell* **2013**, *154*, 1257−1268.
(33) Fitzpatrick, A. W. P.; Debelouchina, G. T.; Bayro, M. J.; Clare, D. K.; Caporini, M. A.; Bajaj, V. S.; Jaroniec, C. P.; Wang, L.; Ladizhansky, V.; Müller, S. A.; et al. Atomic Structure and Hierarchical Assembly of a Cross-β Amyloid Fibril. *Proc. Natl. Acad. Sci. U. S. A.* **2013**, *110*, 5468−5473.
(34) Qiang, W.; Yau, W.-M.; Luo, Y.; Mattson, M. P.; Tycko, R. Antiparallel B-Sheet Architecture in Iowa-Mutant B-Amyloid Fibrils. *Proc. Natl. Acad. Sci. U. S. A.* **2012**, *109*, 4443−4448.
(35) Schütz, A. K.; Soragni, A.; Hornemann, S.; Aguzzi, A.; Ernst, M.; Böckmann, A.; Meier, B. H. The Amyloid-Congo Red Interface at Atomic Resolution. *Angew. Chem., Int. Ed.* **2011**, *50*, 5956−5960.
(36) Van Melckebeke, H.; Wasmer, C.; Lange, A.; Ab, E.; Loquet, A.; Böckmann, A.; Meier, B. H. Atomic-Resolution Three-Dimensional Structure of Het-S(218−289) Amyloid Fibrils by Solid-State NMR Spectroscopy. *J. Am. Chem. Soc.* **2010**, *132*, 13765−13775.
(37) Paravastu, A. K.; Leapman, R. D.; Yau, W. M.; Tycko, R. Molecular Structural Basis for Polymorphism in Alzheimer's Beta-Amyloid Fibrils. *Proc. Natl. Acad. Sci. U. S. A.* **2008**, *105*, 18349−18354.
(38) Madine, J.; Jack, E.; Stockley, P. G.; Radford, S. E.; Serpell, L. C.; Middleton, D. A. Structural Insights into the Polymorphism of Amyloid-Like Fibrils Formed by Region 20−29 of Amylin Revealed by Solid-State NMR and X-Ray Fiber Diffraction. *J. Am. Chem. Soc.* **2008**, *130*, 14990−15001.
(39) Iwata, K.; Fujiwara, T.; Matsuki, Y.; Akutsu, H.; Takahashi, S.; Naiki, H.; Goto, Y. 3D Structure of Amyloid Protofilaments of Beta2-Microglobulin Fragment Probed by Solid-State NMR. *Proc. Natl. Acad. Sci. U. S. A.* **2006**, *103*, 18119−18124.
(40) Ferguson, N.; Becker, J.; Tidow, H.; Tremmel, S.; Sharpe, T. D.; Krause, G.; Flinders, J.; Petrovich, M.; Berriman, J.; Oschkinat, H.; et al. General Structural Motifs of Amyloid Protofilaments. *Proc. Natl. Acad. Sci. U. S. A.* **2006**, *103*, 16248−16253.
(41) Jaroniec, C. P.; MacPhee, C. E.; Bajaj, V. S.; McMahon, M. T.; Dobson, C. M.; Griffin, R. G. High-Resolution Molecular Structure of a Peptide in an Amyloid Fibril Determined by Magic Angle Spinning NMR Spectroscopy. *Proc. Natl. Acad. Sci. U. S. A.* **2004**, *101*, 711−716.
(42) Tycko, R. Molecular Structure of Aggregated Amyloid-B: Insights from Solid State Nuclear Magnetic Resonance. *Cold Spring Harbor Perspect. Med.* **2016**, *6*, a024083.
(43) Meier, B. H.; Riek, R.; Böckmann, A. Emerging Structural Understanding of Amyloid Fibrils by Solid-State NMR. *Trends Biochem. Sci.* **2017**, *42*, 777−787.
(44) van der Wel, P. C. A. Insights into Protein Misfolding and Aggregation Enabled by Solid-State NMR Spectroscopy. *Solid State Nucl. Magn. Reson.* **2017**, *88*, 1−14.
(45) Loquet, A.; El Mammeri, N.; Stanek, J.; Berbon, M.; Bardiaux, B.; Pintacuda, G.; Habenstein, B. 3d Structure Determination of Amyloid Fibrils Using Solid-State NMR Spectroscopy. *Methods* **2018**, *138−139*, 26−38.
(46) Jaroniec, C. P. Two Decades of Progress in Structural and Dynamic Studies of Amyloids by Solid-State NMR. *J. Magn. Reson.* **2019**, *306*, 42−47.
(47) Tycko, R. Solid-State NMR Studies of Amyloid Fibril Structure. *Annu. Rev. Phys. Chem.* **2011**, *62*, 279−299.
(48) Hoyer, W.; Heise, H. In *Amyloid Fibrils and Prefibrillar Aggregates*; Otzen, D., Ed.; Wiley-VCH, 2013; pp 39−61.
(49) Chiti, F.; Dobson, C. M. Protein Misfolding, Functional Amyloid, and Human Disease. *Annu. Rev. Biochem.* **2006**, *75*, 333−366.
(50) Nielsen, J. T.; Bjerring, M.; Jeppesen, M. D.; Pedersen, R. O.; Pedersen, J. M.; Hein, K. L.; Vosegaard, T.; Skrydstrup, T.; Otzen, D. E.; Nielsen, N. C. Unique Identification of Supramolecular Structures in Amyloid Fibrils by Solid-State NMR Spectroscopy. *Angew. Chem., Int. Ed.* **2009**, *48*, 2118−2121.
(51) Schneider, R.; Schumacher, M. C.; Mueller, H.; Nand, D.; Klaukien, V.; Heise, H.; Riedel, D.; Wolf, G.; Behrmann, E.; Raunser, S.; et al. Structural Characterization of Polyglutamine Fibrils by Solid-State NMR Spectroscopy. *J. Mol. Biol.* **2011**, *412*, 121−136.
(52) Hoop, C. L.; Lin, H. K.; Kar, K.; Magyarfalvi, G.; Lamley, J. M.; Boatz, J. C.; Mandal, A.; Lewandowski, J. R.; Wetzel, R.; van der Wel, P. C. Huntingtin Exon 1 Fibrils Feature an Interdigitated β-Hairpin-Based Polyglutamine Core. *Proc. Natl. Acad. Sci. U. S. A.* **2016**, *113*, 1546−1551.
(53) van der Wel, P. C. A.; Lewandowski, J. R.; Griffin, R. G. Structural Characterization of Gnnqqny Amyloid Fibrils by Magic Angle Spinning Nmr. *Biochemistry* **2010**, *49*, 9457−9469.
(54) Shewmaker, F.; Wickner, R. B.; Tycko, R. Amyloid of the Prion Domain of Sup35p Has an in-Register Parallel Beta-Sheet Structure. *Proc. Natl. Acad. Sci. U. S. A.* **2006**, *103*, 19754−19759.

https://doi.org/10.1021/acs.chemrev.1c00196
Chem. Rev. 2021, 121, 8285−8307

(55) Seuring, C.; Verasdonck, J.; Gath, J.; Ghosh, D.; Nespovitaya, N.; Wälti, M. A.; Maji, S. K.; Cadalbert, R.; Güntert, P.; Meier, B. H.; et al. The Three-Dimensional Structure of Human β-Endorphin Amyloid Fibrils. *Nat. Struct. Mol. Biol.* **2020**, *27*, 1178−1184.
(56) Jenkins, J.; Pickersgill, R. The Architecture of Parallel Beta-Helices and Related Folds. *Prog. Biophys. Mol. Biol.* **2001**, *77*, 111−175.
(57) Wasmer, C.; Lange, A.; Van Melckebeke, H.; Siemer, A. B.; Riek, R.; Meier, B. H. Amyloid Fibrils of the Het-S(218−289) Prion Form a β&Solenoid with a Triangular Hydrophobic Core. *Science* **2008**, *319*, 1523−1526.
(58) Sen, A.; Baxa, U.; Simon, M. N.; Wall, J. S.; Sabate, R.; Saupe, S. J.; Steven, A. C. Mass Analysis by Scanning Transmission Electron Microscopy and Electron Diffraction Validate Predictions of Stacked Beta-Solenoid Model of Het-S Prion Fibrils. *J. Biol. Chem.* **2007**, *282*, 5545−5550.
(59) Mizuno, N.; Baxa, U.; Steven, A. C. Structural Dependence of Het-S Amyloid Fibril Infectivity Assessed by Cryoelectron Microscopy. *Proc. Natl. Acad. Sci. U. S. A.* **2011**, *108*, 3252−3257.
(60) Daskalov, A.; Habenstein, B.; Sabaté, R.; Berbon, M.; Martinez, D.; Chaignepain, S.; Coulary-Salin, B.; Hofmann, K.; Loquet, A.; Saupe, S. J. Identification of a Novel Cell Death-Inducing Domain Reveals That Fungal Amyloid-Controlled Programmed Cell Death Is Related to Necroptosis. *Proc. Natl. Acad. Sci. U. S. A.* **2016**, *113*, 2720−2725.
(61) Shewmaker, F.; McGlinchey, R. P.; Thurber, K. R.; McPhie, P.; Dyda, F.; Tycko, R.; Wickner, R. B. The Functional Curli Amyloid Is Not Based on in-Register Parallel Beta-Sheet Structure. *J. Biol. Chem.* **2009**, *284*, 25065−25076.
(62) Schubeis, T.; Yuan, P.; Ahmed, M.; Nagaraj, M.; van Rossum, B.-J.; Ritter, C. Untangling a Repetitive Amyloid Sequence: Correlating Biofilm-Derived and Segmentally Labeled Curli Fimbriae by Solid-State NMR Spectroscopy. *Angew. Chem., Int. Ed.* **2015**, *54*, 14669−14672.
(63) Frederick, K. K.; Michaelis, V. K.; Caporini, M. A.; Andreas, L. B.; Debelouchina, G. T.; Griffin, R. G.; Lindquist, S. Combining DNP NMR with Segmental and Specific Labeling to Study a Yeast Prion Protein Strain That Is Not Parallel in-Register. *Proc. Natl. Acad. Sci. U. S. A.* **2017**, *114*, 3642−3647.
(64) Shewmaker, F.; Kryndushkin, D.; Chen, B.; Tycko, R.; Wickner, R. B. Two Prion Variants of Sup35p Have in-Register Parallel Beta-Sheet Structures, Independent of Hydration. *Biochemistry* **2009**, *48*, 5074−5082.
(65) Ohhashi, Y.; Yamaguchi, Y.; Kurahashi, H.; Kamatari, Y. O.; Sugiyama, S.; Uluca, B.; Piechatzek, T.; Komi, Y.; Shida, T.; Müller, H.; et al. Molecular Basis for Diversification of Yeast Prion Strain Conformation. *Proc. Natl. Acad. Sci. U. S. A.* **2018**, *115*, 2389−2394.
(66) Vázquez-Fernández, E.; Vos, M. R.; Afanasyev, P.; Cebey, L.; Sevillano, A. M.; Vidal, E.; Rosa, I.; Renault, L.; Ramos, A.; Peters, P. J.; et al. The Structural Architecture of an Infectious Mammalian Prion Using Electron Cryomicroscopy. *PLoS Pathog.* **2016**, *12*, No. e1005835.
(67) Wille, H.; Requena, J. The Structure of PrP^{Sc} Prions. *Pathogens* **2018**, *7*, 20.
(68) Kraus, A.; Hoyt, F.; Schwartz, C. L.; Hansen, B.; Hughson, A. G.; Artikis, E.; Race, B.; Caughey, B. Structure of an Infectious Mammalian Prion. *bioRxiv* **2021**, DOI: 10.1101/2021.02.14.431014.
(69) Kollmer, M.; Close, W.; Funk, L.; Rasmussen, J.; Bsoul, A.; Schierhorn, A.; Schmidt, M.; Sigurdson, C. J.; Jucker, M.; Fandrich, M. Cryo-EM Structure and Polymorphism of Abeta Amyloid Fibrils Purified from Alzheimer's Brain Tissue. *Nat. Commun.* **2019**, *10*, 4760.
(70) Ghosh, U.; Thurber, K. R.; Yau, W.-M.; Tycko, R. Molecular Structure of a Prevalent Amyloid-β Fibril Polymorph from Alzheimer's Disease Brain Tissue. *Proc. Natl. Acad. Sci. U. S. A.* **2021**, *118*, No. e2023089118.
(71) Wang, L. Q.; Zhao, K.; Yuan, H. Y.; Wang, Q.; Guan, Z.; Tao, J.; Li, X. N.; Sun, Y.; Yi, C. W.; Chen, J.; et al. Cryo-EM Structure of an Amyloid Fibril Formed by Full-Length Human Prion Protein. *Nat. Struct. Mol. Biol.* **2020**, *27*, 598−602.
(72) Glynn, C.; Sawaya, M. R.; Ge, P.; Gallagher-Jones, M.; Short, C. W.; Bowman, R.; Apostol, M.; Zhou, Z. H.; Eisenberg, D. S.; Rodriguez, J. A. Cryo-EM Structure of a Human Prion Fibril with a Hydrophobic, Protease-Resistant Core. *Nat. Struct. Mol. Biol.* **2020**, *27*, 417−423.
(73) Gallardo, R.; Iadanza, M. G.; Xu, Y.; Heath, G. R.; Foster, R.; Radford, S. E.; Ranson, N. A. Fibril Structures of Diabetes-Related Amylin Variants Reveal a Basis for Surface-Templated Assembly. *Nat. Struct. Mol. Biol.* **2020**, *27*, 1048−1056.
(74) Roder, C.; Kupreichyk, T.; Gremer, L.; Schafer, L. U.; Pothula, K. R.; Ravelli, R. B. G.; Willbold, D.; Hoyer, W.; Schroder, G. F. Cryo-EM Structure of Islet Amyloid Polypeptide Fibrils Reveals Similarities with Amyloid-Beta Fibrils. *Nat. Struct. Mol. Biol.* **2020**, *27*, 660−667.
(75) Cao, Q.; Boyer, D. R.; Sawaya, M. R.; Ge, P.; Eisenberg, D. S. Cryo-EM Structure and Inhibitor Design of Human IAPP (Amylin) Fibrils. *Nat. Struct. Mol. Biol.* **2020**, *27*, 653−659.
(76) Schweighauser, M.; Shi, Y.; Tarutani, A.; Kametani, F.; Murzin, A. G.; Ghetti, B.; Matsubara, T.; Tomita, T.; Ando, T.; Hasegawa, K.; et al. Structures of Alpha-Synuclein Filaments from Multiple System Atrophy. *Nature* **2020**, *585*, 464−469.
(77) Boyer, D. R.; Li, B.; Sun, C.; Fan, W.; Sawaya, M. R.; Jiang, L.; Eisenberg, D. S. Structures of Fibrils Formed by Alpha-Synuclein Hereditary Disease Mutant H50Q Reveal New Polymorphs. *Nat. Struct. Mol. Biol.* **2019**, *26*, 1044−1052.
(78) Lövestam, S.; Schweighauser, M.; Matsubara, T.; Murayama, S.; Tomita, T.; Ando, T.; Hasegawa, K.; Yoshida, M.; Tarutani, A.; Hasegawa, M.; et al. Seeded Assembly in Vitro Does Not Replicate the Structures of A-Synuclein Filaments from Multiple System Atrophy. *FEBS Open Bio* **2021**, *11*, 999−1013.
(79) Arakhamia, T.; Lee, C. E.; Carlomagno, Y.; Duong, D. M.; Kundinger, S. R.; Wang, K.; Williams, D.; DeTure, M.; Dickson, D. W.; Cook, C. N.; et al. Posttranslational Modifications Mediate the Structural Diversity of Tauopathy Strains. *Cell* **2020**, *180*, 633−644.
(80) Hervas, R.; Rau, M. J.; Park, Y.; Zhang, W.; Murzin, A. G.; Fitzpatrick, J. A. J.; Scheres, S. H. W.; Si, K. Cryo-EM Structure of a Neuronal Functional Amyloid Implicated in Memory Persistence in Drosophila. *Science* **2020**, *367*, 1230−1234.
(81) Sun, Y.; Zhao, K.; Xia, W.; Feng, G.; Gu, J.; Ma, Y.; Gui, X.; Zhang, X.; Fang, Y.; Sun, B.; et al. The Nuclear Localization Sequence Mediates Hnrnpa1 Amyloid Fibril Formation Revealed by CryoEM Structure. *Nat. Commun.* **2020**, *11*, 6349.
(82) Lee, M.; Ghosh, U.; Thurber, K. R.; Kato, M.; Tycko, R. Molecular Structure and Interactions within Amyloid-Like Fibrils Formed by a Low-Complexity Protein Sequence from Fus. *Nat. Commun.* **2020**, *11*, 5735.
(83) Lu, J.; Cao, Q.; Hughes, M. P.; Sawaya, M. R.; Boyer, D. R.; Cascio, D.; Eisenberg, D. S. CryoEM Structure of the Low-Complexity Domain of Hnrnpa2 and Its Conversion to Pathogenic Amyloid. *Nat. Commun.* **2020**, *11*, 4090.
(84) Zhao, K.; Lim, Y. J.; Liu, Z.; Long, H.; Sun, Y.; Hu, J. J.; Zhao, C.; Tao, Y.; Zhang, X.; Li, D.; et al. Parkinson's Disease-Related Phosphorylation at Tyr39 Rearranges Alpha-Synuclein Amyloid Fibril Structure Revealed by Cryo-Em. *Proc. Natl. Acad. Sci. U. S. A.* **2020**, *117*, 20305−20315.
(85) Sun, Y.; Hou, S.; Zhao, K.; Long, H.; Liu, Z.; Gao, J.; Zhang, Y.; Su, X. D.; Li, D.; Liu, C. Cryo-Em Structure of Full-Length Alpha-Synuclein Amyloid Fibril with Parkinson's Disease Familial A53T Mutation. *Cell Res.* **2020**, *30*, 360−362.
(86) Boyer, D. R.; Li, B.; Sun, C.; Fan, W.; Zhou, K.; Hughes, M. P.; Sawaya, M. R.; Jiang, L.; Eisenberg, D. S. The Alpha-Synuclein Hereditary Mutation E46k Unlocks a More Stable, Pathogenic Fibril Structure. *Proc. Natl. Acad. Sci. U. S. A.* **2020**, *117*, 3592−3602.
(87) Zhang, W.; Tarutani, A.; Newell, K. L.; Murzin, A. G.; Matsubara, T.; Falcon, B.; Vidal, R.; Garringer, H. J.; Shi, Y.; Ikeuchi, T.; et al. Novel Tau Filament Fold in Corticobasal Degeneration. *Nature* **2020**, *580*, 283−287.

https://doi.org/10.1021/acs.chemrev.1c00196
Chem. Rev. 2021, 121, 8285−8307

(88) Guerrero-Ferreira, R.; Taylor, N. M. I.; Arteni, A.-A.; Kumari, P.; Mona, D.; Ringler, P.; Britschgi, M.; Lauer, M. E.; Makky, A.; Verasdonck, J.; et al. Two New Polymorphic Structures of Human Full-Length Alpha-Synuclein Fibrils Solved by Cryo-Electron Microscopy. *eLife* **2019**, *8*, No. e48907.
(89) Schmidt, M.; Wiese, S.; Adak, V.; Engler, J.; Agarwal, S.; Fritz, G.; Westermark, P.; Zacharias, M.; Fandrich, M. Cryo-Em Structure of a Transthyretin-Derived Amyloid Fibril from a Patient with Hereditary Attr Amyloidosis. *Nat. Commun.* **2019**, *10*, 5008.
(90) Ni, X.; McGlinchey, R. P.; Jiang, J.; Lee, J. C. Structural Insights into Alpha-Synuclein Fibril Polymorphism: Effects of Parkinson's Disease-Related C-Terminal Truncations. *J. Mol. Biol.* **2019**, *431*, 3913−3919.
(91) Roder, C.; Vettore, N.; Mangels, L. N.; Gremer, L.; Ravelli, R. B. G.; Willbold, D.; Hoyer, W.; Buell, A. K.; Schroder, G. F. Atomic Structure of PI3-Kinase SH3 Amyloid Fibrils by Cryo-Electron Microscopy. *Nat. Commun.* **2019**, *10*, 3754.
(92) Cao, Q.; Boyer, D. R.; Sawaya, M. R.; Ge, P.; Eisenberg, D. S. Cryo-Em Structures of Four Polymorphic Tdp-43 Amyloid Cores. *Nat. Struct. Mol. Biol.* **2019**, *26*, 619−627.
(93) Radamaker, L.; Lin, Y. H.; Annamalai, K.; Huhn, S.; Hegenbart, U.; Schonland, S. O.; Fritz, G.; Schmidt, M.; Fandrich, M. Cryo-EM Structure of a Light Chain-Derived Amyloid Fibril from a Patient with Systemic Al Amyloidosis. *Nat. Commun.* **2019**, *10*, 1103.
(94) Falcon, B.; Zivanov, J.; Zhang, W.; Murzin, A. G.; Garringer, H. J.; Vidal, R.; Crowther, R. A.; Newell, K. L.; Ghetti, B.; Goedert, M.; et al. Novel Tau Filament Fold in Chronic Traumatic Encephalopathy Encloses Hydrophobic Molecules. *Nature* **2019**, *568*, 420−423.
(95) Swuec, P.; Lavatelli, F.; Tasaki, M.; Paissoni, C.; Rognoni, P.; Maritan, M.; Brambilla, F.; Milani, P.; Mauri, P.; Camilloni, C.; et al. Cryo-EM Structure of Cardiac Amyloid Fibrils from an Immunoglobulin Light Chain Al Amyloidosis Patient. *Nat. Commun.* **2019**, *10*, 1269.
(96) Liberta, F.; Loerch, S.; Rennegarbe, M.; Schierhorn, A.; Westermark, P.; Westermark, G. T.; Hazenberg, B. P. C.; Grigorieff, N.; Fandrich, M.; Schmidt, M. Cryo-EM Fibril Structures from Systemic AA Amyloidosis Reveal the Species Complementarity of Pathological Amyloids. *Nat. Commun.* **2019**, *10*, 1104.
(97) Zhang, W.; Falcon, B.; Murzin, A. G.; Fan, J.; Crowther, R. A.; Goedert, M.; Scheres, S. H. Heparin-Induced Tau Filaments Are Polymorphic and Differ from Those in Alzheimer's and Pick's Diseases. *eLife* **2019**, *8*, e43584.
(98) Iadanza, M. G.; Silvers, R.; Boardman, J.; Smith, H. I.; Karamanos, T. K.; Debelouchina, G. T.; Su, Y.; Griffin, R. G.; Ranson, N. A.; Radford, S. E. The Structure of a β2-Microglobulin Fibril Suggests a Molecular Basis for Its Amyloid Polymorphism. *Nat. Commun.* **2018**, *9*, 4517.
(99) Falcon, B.; Zhang, W.; Schweighauser, M.; Murzin, A. G.; Vidal, R.; Garringer, H. J.; Ghetti, B.; Scheres, S. H. W.; Goedert, M. Tau Filaments from Multiple Cases of Sporadic and Inherited Alzheimer's Disease Adopt a Common Fold. *Acta Neuropathol.* **2018**, *136*, 699−708.
(100) Falcon, B.; Zhang, W.; Murzin, A. G.; Murshudov, G.; Garringer, H. J.; Vidal, R.; Crowther, R. A.; Ghetti, B.; Scheres, S. H. W.; Goedert, M. Structures of Filaments from Pick's Disease Reveal a Novel Tau Protein Fold. *Nature* **2018**, *561*, 137−140.
(101) Li, B.; Ge, P.; Murray, K. A.; Sheth, P.; Zhang, M.; Nair, G.; Sawaya, M. R.; Shin, W. S.; Boyer, D. R.; Ye, S.; et al. Cryo-EM of Full-Length Alpha-Synuclein Reveals Fibril Polymorphs with a Common Structural Kernel. *Nat. Commun.* **2018**, *9*, 3609.
(102) Guerrero-Ferreira, R.; Taylor, N. M. I.; Mona, D.; Ringler, P.; Lauer, M. E.; Riek, R.; Britschgi, M.; Stahlberg, H. Cryo-EM Structure of Alpha-Synuclein Fibrils. *eLife* **2018**, *7*, No. e36402.
(103) Li, Y.; Zhao, C.; Luo, F.; Liu, Z.; Gui, X.; Luo, Z.; Zhang, X.; Li, D.; Liu, C.; Li, X. Amyloid Fibril Structure of Alpha-Synuclein Determined by Cryo-Electron Microscopy. *Cell Res.* **2018**, *28*, 897−903.
(104) Tycko, R. Physical and Structural Basis for Polymorphism in Amyloid Fibrils. *Protein Sci.* **2014**, *23*, 1528−1539.
(105) Petkova, A. T.; Leapman, R. D.; Guo, Z.; Yau, W.-M.; Mattson, M. P.; Tycko, R. Self-Propagating, Molecular-Level Polymorphism in Alzheimer's β-Amyloid Fibrils. *Science* **2005**, *307*, 262−265.
(106) Sachse, C.; Fändrich, M.; Grigorieff, N. Paired B-Sheet Structure of an Aβ(1−40) Amyloid Fibril Revealed by Electron Microscopy. *Proc. Natl. Acad. Sci. U. S. A.* **2008**, *105*, 7462−7466.
(107) Schmidt, M.; Sachse, C.; Richter, W.; Xu, C.; Fandrich, M.; Grigorieff, N. Comparison of Alzheimer a Beta(1−40) and a Beta(1−42) Amyloid Fibrils Reveals Similar Protofilament Structures. *Proc. Natl. Acad. Sci. U. S. A.* **2009**, *106*, 19813−19818.
(108) Qiang, W.; Yau, W.-M.; Lu, J.-X.; Collinge, J.; Tycko, R. Structural Variation in Amyloid-β Fibrils from Alzheimer's Disease Clinical Subtypes. *Nature* **2017**, *541*, 217−221.
(109) Heise, H.; Hoyer, W.; Becker, S.; Andronesi, O. C.; Riedel, D.; Baldus, M. Molecular-Level Secondary Structure, Polymorphism, and Dynamics of Full-Length (-Synuclein Fibrils Studied by Solid-State NMR. *Proc. Natl. Acad. Sci. U. S. A.* **2005**, *102*, 15871−15876.
(110) Bousset, L.; Pieri, L.; Ruiz-Arlandis, G.; Gath, J.; Jensen, P. H.; Habenstein, B.; Madiona, K.; Olieric, V.; Böckmann, A.; Meier, B. H.; et al. Structural and Functional Characterization of Two Alpha-Synuclein Strains. *Nat. Commun.* **2013**, *4*, 2575.
(111) Seuring, C.; Verasdonck, J.; Ringler, P.; Cadalbert, R.; Stahlberg, H.; Böckmann, A.; Meier, B. H.; Riek, R. Amyloid Fibril Polymorphism: Almost Identical on the Atomic Level, Mesoscopically Very Different. *J. Phys. Chem. B* **2017**, *121*, 1783−1792.
(112) Close, W.; Neumann, M.; Schmidt, A.; Hora, M.; Annamalai, K.; Schmidt, M.; Reif, B.; Schmidt, V.; Grigorieff, N.; Fändrich, M. Physical Basis of Amyloid Fibril Polymorphism. *Nat. Commun.* **2018**, *9*, 699.
(113) van der Wel, P. C.; Lewandowski, J. R.; Griffin, R. G. Structural Characterization of GNNQQNY Amyloid Fibrils by Magic Angle Spinning NMR. *Biochemistry* **2010**, *49*, 9457−9469.
(114) Hoop, C. L.; Lin, H.-K.; Kar, K.; Hou, Z.; Poirier, M. A.; Wetzel, R.; van der Wel, P. C. A. Polyglutamine Amyloid Core Boundaries and Flanking Domain Dynamics in Huntingtin Fragment Fibrils Determined by Solid-State Nuclear Magnetic Resonance. *Biochemistry* **2014**, *53*, 6653−6666.
(115) Isas, J. M.; Langen, R.; Siemer, A. B. Solid-State Nuclear Magnetic Resonance on the Static and Dynamic Domains of Huntingtin Exon-1 Fibrils. *Biochemistry* **2015**, *54*, 3942−3949.
(116) Lopez del Amo, J. M.; Schmidt, M.; Fink, U.; Dasari, M.; Fändrich, M.; Reif, B. An Asymmetric Dimer as the Basic Subunit in Alzheimer's Disease Amyloid β Fibrils. *Angew. Chem., Int. Ed.* **2012**, *51*, 6136−6139.
(117) Noji, M.; Samejima, T.; Yamaguchi, K.; So, M.; Yuzu, K.; Chatani, E.; Akazawa-Ogawa, Y.; Hagihara, Y.; Kawata, Y.; Ikenaka, K.; et al. Breakdown of Supersaturation Barrier Links Protein Folding to Amyloid Formation. *Commun. Biol.* **2021**, *4*, 120.
(118) Wolff, M.; Unuchek, D.; Zhang, B.; Gordeliy, V.; Willbold, D.; Nagel-Steger, L. Amyloid β Oligomeric Species Present in the Lag Phase of Amyloid Formation. *PLoS One* **2015**, *10*, No. e0127865.
(119) Wolff, M.; Zhang-Haagen, B.; Decker, C.; Barz, B.; Schneider, M.; Biehl, R.; Radulescu, A.; Strodel, B.; Willbold, D.; Nagel-Steger, L. Aβ42 Pentamers/Hexamers Are the Smallest Detectable Oligomers in Solution. *Sci. Rep.* **2017**, *7*, 2493.
(120) Michaels, T. C. T.; Šarić, A.; Habchi, J.; Chia, S.; Meisl, G.; Vendruscolo, M.; Dobson, C. M.; Knowles, T. P. J. Chemical Kinetics for Bridging Molecular Mechanisms and Macroscopic Measurements of Amyloid Fibril Formation. *Annu. Rev. Phys. Chem.* **2018**, *69*, 273−298.
(121) Arosio, P.; Knowles, T. P.; Linse, S. On the Lag Phase in Amyloid Fibril Formation. *Phys. Chem. Chem. Phys.* **2015**, *17*, 7606−7618.
(122) Michaels, T. C. T.; Weber, C. A.; Mahadevan, L. Optimal Control Strategies for Inhibition of Protein Aggregation. *Proc. Natl. Acad. Sci. U. S. A.* **2019**, *116*, 14593−14598.

https://doi.org/10.1021/acs.chemrev.1c00196
Chem. Rev. 2021, 121, 8285−8307

(123) Meisl, G.; Knowles, T. P.; Klenerman, D. The Molecular Processes Underpinning Prion-Like Spreading and Seed Amplification in Protein Aggregation. *Curr. Opin. Neurobiol.* **2020**, *61*, 58−64.
(124) Hepler, R. W.; Grimm, K. M.; Nahas, D. D.; Breese, R.; Dodson, E. C.; Acton, P.; Keller, P. M.; Yeager, M.; Wang, H.; Shughrue, P.; et al. Solution State Characterization of Amyloid Beta-Derived Diffusible Ligands. *Biochemistry* **2006**, *45*, 15157−15167.
(125) Yu, L.; Edalji, R.; Harlan, J. E.; Holzman, T. F.; Lopez, A. P.; Labkovsky, B.; Hillen, H.; Barghorn, S.; Ebert, U.; Richardson, P. L.; et al. Structural Characterization of a Soluble Amyloid Beta-Peptide Oligomer. *Biochemistry* **2009**, *48*, 1870−1877.
(126) Ciudad, S.; Puig, E.; Botzanowski, T.; Meigooni, M.; Arango, A. S.; Do, J.; Mayzel, M.; Bayoumi, M.; Chaignepain, S.; Maglia, G.; et al. Aβ(1−42) Tetramer and Octamer Structures Reveal Edge Conductivity Pores as a Mechanism for Membrane Damage. *Nat. Commun.* **2020**, *11*, 3014.
(127) Sang, J. C.; Lee, J. E.; Dear, A. J.; De, S.; Meisl, G.; Thackray, A. M.; Bujdoso, R.; Knowles, T. P. J.; Klenerman, D. Direct Observation of Prion Protein Oligomer Formation Reveals an Aggregation Mechanism with Multiple Conformationally Distinct Species. *Chem. Sci.* **2019**, *10*, 4588−4597.
(128) Sahoo, B. R.; Cox, S. J.; Ramamoorthy, A. High-Resolution Probing of Early Events in Amyloid-B Aggregation Related to Alzheimer's Disease. *Chem. Commun. (Cambridge, U. K.)* **2020**, *56*, 4627−4639.
(129) König, A. S.; Rösener, N. S.; Gremer, L.; Tusche, M.; Flender, D.; Reinartz, E.; Hoyer, W.; Neudecker, P.; Willbold, D.; Heise, H. Structural Details of Amyloid B Oligomers in Complex with Human Prion Protein as Revealed by Solid-State MAS NMR Spectroscopy. *J. Biol. Chem.* **2021**, *296*, 100499.
(130) Kostylev, M. A.; Tuttle, M. D.; Lee, S.; Klein, L. E.; Takahashi, H.; Cox, T. O.; Gunther, E. C.; Zilm, K. W.; Strittmatter, S. M. Liquid and Hydrogel Phases of Prp(C) Linked to Conformation Shifts and Triggered by Alzheimer's Amyloid-β Oligomers. *Mol. Cell* **2018**, *72*, 426−443.
(131) Muchowska, K. B.; Varma, S. J.; Moran, J. Nonenzymatic Metabolic Reactions and Life's Origins. *Chem. Rev.* **2020**, *120*, 7708−7744.
(132) Gao, Y.; Guo, C.; Watzlawik, J. O.; Randolph, P. S.; Lee, E. J.; Huang, D.; Stagg, S. M.; Zhou, H.-X.; Rosenberry, T. L.; Paravastu, A. K. Out-of-Register Parallel B-Sheets and Antiparallel β-Sheets Coexist in 150-kDa Oligomers Formed by Amyloid-β(1−42). *J. Mol. Biol.* **2020**, *432*, 4388−4407.
(133) Jaunmuktane, Z.; Mead, S.; Ellis, M.; Wadsworth, J. D.; Nicoll, A. J.; Kenny, J.; Launchbury, F.; Linehan, J.; Richard-Loendt, A.; Walker, A. S.; et al. Evidence for Human Transmission of Amyloid-B Pathology and Cerebral Amyloid Angiopathy. *Nature* **2015**, *525*, 247−250.
(134) Jucker, M.; Walker, L. C. Propagation and Spread of Pathogenic Protein Assemblies in Neurodegenerative Diseases. *Nat. Neurosci.* **2018**, *21*, 1341−1349.
(135) Walker, L. C. Prion-Like Mechanisms in Alzheimer Disease. *Handb. Clin. Neurol.* **2018**, *153*, 303−319.
(136) Walker, L. C.; Jucker, M. Neurodegenerative Diseases: Expanding the Prion Concept. *Annu. Rev. Neurosci.* **2015**, *38*, 87−103.
(137) Walker, L. C.; LeVine, H., 3rd Corruption and Spread of Pathogenic Proteins in Neurodegenerative Diseases. *J. Biol. Chem.* **2012**, *287*, 33109−33115.
(138) Peng, C.; Trojanowski, J. Q.; Lee, V. M. Protein Transmission in Neurodegenerative Disease. *Nat. Rev. Neurol.* **2020**, *16*, 199−212.
(139) Davis, A. A.; Leyns, C. E. G.; Holtzman, D. M. Intercellular Spread of Protein Aggregates in Neurodegenerative Disease. *Annu. Rev. Cell Dev. Biol.* **2018**, *34*, 545−568.
(140) Iwasaki, Y. The Braak Hypothesis in Prion Disease with a Focus on Creutzfeldt-Jakob Disease. *Neuropathology* **2020**, *40*, 436−449.
(141) Kumar, H.; Udgaonkar, J. B. Mechanistic Approaches to Understand the Prion-Like Propagation of Aggregates of the Human Tau Protein. *Biochim. Biophys. Acta, Proteins Proteomics* **2019**, *1867*, 922−932.
(142) Watts, J. C.; Prusiner, S. B. B-Amyloid Prions and the Pathobiology of Alzheimer's Disease. *Cold Spring Harbor Perspect. Med.* **2018**, *8*, a023507.
(143) Asher, D. M.; Belay, E.; Bigio, E.; Brandner, S.; Brubaker, S. A.; Caughey, B.; Clark, B.; Damon, I.; Diamond, M.; Freund, M.; et al. Risk of Transmissibility from Neurodegenerative Disease-Associated Proteins: Experimental Knowns and Unknowns. *J. Neuropathol. Exp. Neurol.* **2020**, *79*, 1141−1146.
(144) Duyckaerts, C.; Clavaguera, F.; Potier, M. C. The Prion-Like Propagation Hypothesis in Alzheimer's and Parkinson's Disease. *Curr. Opin. Neurol.* **2019**, *32*, 266−271.
(145) Chu, D.; Liu, F. Pathological Changes of Tau Related to Alzheimer's Disease. *ACS Chem. Neurosci.* **2019**, *10*, 931−944.
(146) Watts, J. C.; Condello, C.; Stöhr, J.; Oehler, A.; Lee, J.; DeArmond, S. J.; Lannfelt, L.; Ingelsson, M.; Giles, K.; Prusiner, S. B. Serial Propagation of Distinct Strains of Aβ Prions from Alzheimer's Disease Patients. *Proc. Natl. Acad. Sci. U. S. A.* **2014**, *111*, 10323−10328.
(147) Alpaugh, M.; Cicchetti, F. Huntington's Disease: Lessons from Prion Disorders. *J. Neurol.* **2021**, DOI: 10.1007/s00415-021-10418-8.
(148) Xu, H.; O'Reilly, M.; Gibbons, G. S.; Changolkar, L.; McBride, J. D.; Riddle, D. M.; Zhang, B.; Stieber, A.; Nirschl, J.; Kim, S. J.; et al. In Vitro Amplification of Pathogenic Tau Conserves Disease-Specific Bioactive Characteristics. *Acta Neuropathol.* **2021**, *141*, 193−215.
(149) Woerman, A. L.; Oehler, A.; Kazmi, S. A.; Lee, J.; Halliday, G. M.; Middleton, L. T.; Gentleman, S. M.; Mordes, D. A.; Spina, S.; Grinberg, L. T.; et al. Multiple System Atrophy Prions Retain Strain Specificity after Serial Propagation in Two Different Tg-(SNCA*A53T) Mouse Lines. *Acta Neuropathol.* **2019**, *137*, 437−454.
(150) Friesen, M.; Meyer-Luehmann, M. Aβ Seeding as a Tool to Study Cerebral Amyloidosis and Associated Pathology. *Front. Mol. Neurosci.* **2019**, *12*, 233.
(151) Brunello, C. A.; Merezhko, M.; Uronen, R. L.; Huttunen, H. J. Mechanisms of Secretion and Spreading of Pathological Tau Protein. *Cell. Mol. Life Sci.* **2020**, *77*, 1721−1744.
(152) Scialò, C.; De Cecco, E.; Manganotti, P.; Legname, G. Prion and Prion-Like Protein Strains: Deciphering the Molecular Basis of Heterogeneity in Neurodegeneration. *Viruses* **2019**, *11*, 261.
(153) Gary, C.; Lam, S.; Hérard, A. S.; Koch, J. E.; Petit, F.; Gipchtein, P.; Sawiak, S. J.; Caillierez, R.; Eddarkaoui, S.; Colin, M.; et al. Encephalopathy Induced by Alzheimer Brain Inoculation in a Non-Human Primate. *Acta Neuropathol. Commun.* **2019**, *7*, 126.
(154) Hérard, A. S.; Petit, F.; Gary, C.; Guillermier, M.; Boluda, S.; Garin, C. M.; Lam, S.; Dhenain, M. Induction of Amyloid-B Deposits from Serially Transmitted, Histologically Silent, Aβ Seeds Issued from Human Brains. *Acta Neuropathol. Commun.* **2020**, *8*, 205.
(155) Gomez-Gutierrez, R.; Morales, R. The Prion-Like Phenomenon in Alzheimer's Disease: Evidence of Pathology Transmission in Humans. *PLoS Pathog.* **2020**, *16*, No. e1009004.
(156) Aguzzi, A.; De Cecco, E. Shifts and Drifts in Prion Science. *Science* **2020**, *370*, 32−34.
(157) Goedert, M. Tau Proteinopathies and the Prion Concept. *Prog. Mol. Biol. Transl. Sci.* **2020**, *175*, 239−259.
(158) Catania, M.; Di Fede, G. One or More β-Amyloid(s)? New Insights into the Prion-Like Nature of Alzheimer's Disease. *Prog. Mol. Biol. Transl. Sci.* **2020**, *175*, 213−237.
(159) Spagnolli, G.; Requena, J. R.; Biasini, E. Understanding Prion Structure and Conversion. *Prog. Mol. Biol. Transl. Sci.* **2020**, *175*, 19−30.
(160) McAlary, L.; Yerbury, J. J.; Cashman, N. R. The Prion-Like Nature of Amyotrophic Lateral Sclerosis. *Prog. Mol. Biol. Transl. Sci.* **2020**, *175*, 261−296.
(161) Holec, S. A. M.; Block, A. J.; Bartz, J. C. The Role of Prion Strain Diversity in the Development of Successful Therapeutic Treatments. *Prog. Mol. Biol. Transl. Sci.* **2020**, *175*, 77−119.

https://doi.org/10.1021/acs.chemrev.1c00196
Chem. Rev. 2021, 121, 8285−8307

(162) Lau, A.; So, R. W. L.; Lau, H. H. C.; Sang, J. C.; Ruiz-Riquelme, A.; Fleck, S. C.; Stuart, E.; Menon, S.; Visanji, N. P.; Meisl, G.; et al. A-Synuclein Strains Target Distinct Brain Regions and Cell Types. *Nat. Neurosci.* **2020**, *23*, 21−31.
(163) Lau, H. H. C.; Ingelsson, M.; Watts, J. C. The Existence of Aβ Strains and Their Potential for Driving Phenotypic Heterogeneity in Alzheimer's Disease. *Acta Neuropathol.* **2020**, DOI: 10.1007/s00401-020-02201-2.
(164) Walker, L. C.; Diamond, M. I.; Duff, K. E.; Hyman, B. T. Mechanisms of Protein Seeding in Neurodegenerative Diseases. *JAMA Neurol.* **2013**, *70*, 304−310.
(165) Kutzsche, J.; Jürgens, D.; Willuweit, A.; Adermann, K.; Fuchs, C.; Simons, S.; Windisch, M.; Hümpel, M.; Rossberg, W.; Wolzt, M.; et al. Safety and Pharmacokinetics of the Orally Available Antiprionic Compound PRI-002: A Single and Multiple Ascending Dose Phase I Study. *Alzheimers Dement,* **2020**, *6*, No. e12001.
(166) Willbold, D.; Kutzsche, J. Do We Need Anti-Prion Compounds to Treat Alzheimer's Disease? *Molecules* **2019**, *24*, 2237.
(167) Condello, C.; DeGrado, W. F.; Prusiner, S. B. Prion Biology: Implications for Alzheimer's Disease Therapeutics. *Lancet Neurol.* **2020**, *19*, 802−803.
(168) Seubert, P.; Vigo-Pelfrey, C.; Esch, F.; Lee, M.; Dovey, H.; Davis, D.; Sinha, S.; Schiossmacher, M.; Whaley, J.; Swindlehurst, C.; et al. Isolation and Quantification of Soluble Alzheimer's β-Peptide from Biological Fluids. *Nature* **1992**, *359*, 325−327.
(169) Galasko, D.; Chang, L.; Motter, R.; Clark, C. M.; Kaye, J.; Knopman, D.; Thomas, R.; Kholodenko, D.; Schenk, D.; Lieberburg, I.; et al. High Cerebrospinal Fluid Tau and Low Amyloid Beta42 Levels in the Clinical Diagnosis of Alzheimer Disease and Relation to Apolipoprotein E Genotype. *Arch. Neurol.* **1998**, *55*, 937−945.
(170) Andreasen, N.; Hesse, C.; Davidsson, P.; Minthon, L.; Wallin, A.; Winblad, B.; Vanderstichele, H.; Vanmechelen, E.; Blennow, K. Cerebrospinal Fluid Beta-Amyloid(1−42) in Alzheimer Disease: Differences between Early- and Late-Onset Alzheimer Disease and Stability During the Course of Disease. *Arch. Neurol.* **1999**, *56*, 673−680.
(171) Strozyk, D.; Blennow, K.; White, L. R.; Launer, L. J. Csf Abeta 42 Levels Correlate with Amyloid-Neuropathology in a Population-Based Autopsy Study. *Neurology* **2003**, *60*, 652−656.
(172) Brody, D. L.; Magnoni, S.; Schwetye, K. E.; Spinner, M. L.; Esparza, T. J.; Stocchetti, N.; Zipfel, G. J.; Holtzman, D. M. Amyloid-Beta Dynamics Correlate with Neurological Status in the Injured Human Brain. *Science* **2008**, *321*, 1221−1224.
(173) Fjorback, W. A.; Varming, K.; Jensen, H. P. Determination of A-Synuclein Concentration in Human Plasma Using Elisa. *Scand. J. Clin. Lab. Invest.* **2007**, *67*, 431−435.
(174) Mollenhauer, B.; Locascio, J. J.; Schulz-Schaeffer, W.; Sixel-Döring, F.; Trenkwalder, C.; Schlossmacher, M. G. A-Synuclein and Tau Concentrations in Cerebrospinal Fluid of Patients Presenting with Parkinsonism: A Cohort Study. *Lancet Neurol.* **2011**, *10*, 230−240.
(175) Nakazato, M.; Asai, J.; Kangawa, K.; Matsukura, S.; Matsuo, H. Establishment of Radioimmunoassay for Human Islet Amyloid Polypeptide and Its Tissue Content and Plasma Concentration. *Biochem. Biophys. Res. Commun.* **1989**, *164*, 394−399.
(176) Butler, P. C.; Chou, J.; Carter, W. B.; Wang, Y. N.; Bu, B. H.; Chang, D.; Chang, J. K.; Rizza, R. A. Effects of Meal Ingestion on Plasma Amylin Concentration in Niddm and Nondiabetic Humans. *Diabetes* **1990**, *39*, 752−756.
(177) Höppener, J. W.; Verbeek, J. S.; de Koning, E. J.; Oosterwijk, C.; van Hulst, K. L.; Visser-Vernooy, H. J.; Hofhuis, F. M.; van Gaalen, S.; Berends, M. J.; Hackeng, W. H.; et al. Chronic Overproduction of Islet Amyloid Polypeptide/Amylin in Transgenic Mice: Lysosomal Localization of Human Islet Amyloid Polypeptide and Lack of Marked Hyperglycaemia or Hyperinsulinaemia. *Diabetologia* **1993**, *36*, 1258−1265.
(178) Hassink, G. C.; Raiss, C. C.; Segers-Nolten, I. M. J.; van Wezel, R. J. A.; Subramaniam, V.; le Feber, J.; Claessens, M. Exogenous A-Synuclein Hinders Synaptic Communication in Cultured Cortical Primary Rat Neurons. *PLoS One* **2018**, *13*, No. e0193763.
(179) Iwai, A.; Masliah, E.; Yoshimoto, M.; Ge, N.; Flanagan, L.; Rohan de Silva, H. A.; Kittel, A.; Saitoh, T. The Precursor Protein of Non-a Beta Component of Alzheimer's Disease Amyloid Is a Presynaptic Protein of the Central Nervous System. *Neuron* **1995**, *14*, 467−475.
(180) Raleigh, D.; Zhang, X.; Hastoy, B.; Clark, A. The B-Cell Assassin: IAPP Cytotoxicity. *J. Mol. Endocrinol.* **2017**, *59*, R121−R140.
(181) Garzon-Rodriguez, W.; Sepulveda-Becerra, M.; Milton, S.; Glabe, C. G. Soluble Amyloid Abeta-(1−40) Exists as a Stable Dimer at Low Concentrations. *J. Biol. Chem.* **1997**, *272*, 21037−21044.
(182) Sabaté, R.; Estelrich, J. Evidence of the Existence of Micelles in the Fibrillogenesis of B-Amyloid Peptide. *J. Phys. Chem. B* **2005**, *109*, 11027−11032.
(183) Chimon, S.; Shaibat, M. A.; Jones, C. R.; Calero, D. C.; Aizezi, B.; Ishii, Y. Evidence of Fibril-Like β-Sheet Structures in a Neurotoxic Amyloid Intermediate of Alzheimer's β-Amyloid. *Nat. Struct. Mol. Biol.* **2007**, *14*, 1157−1164.
(184) Ono, K.; Condron, M. M.; Teplow, D. B. Structure-Neurotoxicity Relationships of Amyloid β-Protein Oligomers. *Proc. Natl. Acad. Sci. U. S. A.* **2009**, *106*, 14745−14750.
(185) Bernstein, S. L.; Dupuis, N. F.; Lazo, N. D.; Wyttenbach, T.; Condron, M. M.; Bitan, G.; Teplow, D. B.; Shea, J. E.; Ruotolo, B. T.; Robinson, C. V.; et al. Amyloid-β Protein Oligomerization and the Importance of Tetramers and Dodecamers in the Aetiology of Alzheimer's Disease. *Nat. Chem.* **2009**, *1*, 326−331.
(186) Lee, J.; Culyba, E. K.; Powers, E. T.; Kelly, J. W. Amyloid-β Forms Fibrils by Nucleated Conformational Conversion of Oligomers. *Nat. Chem. Biol.* **2011**, *7*, 602−609.
(187) Novo, M.; Freire, S.; Al-Soufi, W. Critical Aggregation Concentration for the Formation of Early Amyloid-β (1−42) Oligomers. *Sci. Rep.* **2018**, *8*, 1783.
(188) Itzhaki, R. F. Corroboration of a Major Role for Herpes Simplex Virus Type 1 in Alzheimer's Disease. *Front. Aging Neurosci.* **2018**, *10*, 324.
(189) Itzhaki, R. F. A Turning Point in Alzheimer's Disease: Microbes Matter. *J. Alzheimer's Dis.* **2019**, *72*, 977−980.
(190) Itzhaki, R. F.; Golde, T. E.; Heneka, M. T.; Readhead, B. Do Infections Have a Role in the Pathogenesis of Alzheimer Disease? *Nat. Rev. Neurol.* **2020**, *16*, 193−197.
(191) Li, L.; Liang, J.; Fu, H. An Update on the Association between Traumatic Brain Injury and Alzheimer's Disease: Focus on Tau Pathology and Synaptic Dysfunction. *Neurosci. Biobehav. Rev.* **2021**, *120*, 372−386.
(192) Maigler, K. C.; Buhr, T. J.; Park, C. S.; Miller, S. A.; Kozlowski, D. A.; Marr, R. A. Assessment of the Effects of Altered Amyloid-Beta Clearance on Behavior Following Repeat Closed-Head Brain Injury in Amyloid-Beta Precursor Protein Humanized Mice. *J. Neurotrauma* **2021**, *38*, 665−676.
(193) Patterson, B. W.; Elbert, D. L.; Mawuenyega, K. G.; Kasten, T.; Ovod, V.; Ma, S.; Xiong, C.; Chott, R.; Yarasheski, K.; Sigurdson, W.; et al. Age and Amyloid Effects on Human Central Nervous System Amyloid-Beta Kinetics. *Ann. Neurol.* **2015**, *78*, 439−453.
(194) Uauy, R.; Winterer, J. C.; Bilmazes, C.; Haverberg, L. N.; Scrimshaw, N. S.; Munro, H. N.; Young, V. R. The Changing Pattern of Whole Body Protein Metabolism in Aging Humans. *J. Gerontol.* **1978**, *33*, 663−671.
(195) Fu, A.; Nair, K. S. Age Effect on Fibrinogen and Albumin Synthesis in Humans. *American Journal of Physiology-Endocrinology and Metabolism* **1998**, *275*, E1023−E1030.
(196) Bateman, R. J.; Xiong, C.; Benzinger, T. L.; Fagan, A. M.; Goate, A.; Fox, N. C.; Marcus, D. S.; Cairns, N. J.; Xie, X.; Blazey, T. M.; et al. Clinical and Biomarker Changes in Dominantly Inherited Alzheimer's Disease. *N. Engl. J. Med.* **2012**, *367*, 795−804.
(197) Bansal, A.; Schmidt, M.; Rennegarbe, M.; Haupt, C.; Liberta, F.; Stecher, S.; Puscalau-Girtu, I.; Biedermann, A.; Fändrich, M. Aa

Amyloid Fibrils from Diseased Tissue Are Structurally Different from in Vitro Formed Saa Fibrils. *Nat. Commun.* **2021**, *12*, 1013.
(198) Annamalai, K.; Liberta, F.; Vielberg, M.-T.; Close, W.; Lilie, H.; Gührs, K.-H.; Schierhorn, A.; Koehler, R.; Schmidt, A.; Haupt, C.; et al. Common Fibril Structures Imply Systemically Conserved Protein Misfolding Pathways in Vivo. *Angew. Chem., Int. Ed.* **2017**, *56*, 7510−7514.
(199) Radamaker, L.; Baur, J.; Huhn, S.; Haupt, C.; Hegenbart, U.; Schönland, S.; Bansal, A.; Schmidt, M.; Fändrich, M. Cryo-Em Reveals Structural Breaks in a Patient-Derived Amyloid Fibril from Systemic Al Amyloidosis. *Nat. Commun.* **2021**, *12*, 875.
(200) Schweighauser, M.; Shi, Y.; Tarutani, A.; Kametani, F.; Murzin, A. G.; Ghetti, B.; Matsubara, T.; Tomita, T.; Ando, T.; Hasegawa, K.; et al. Structures of α-Synuclein Filaments from Multiple System Atrophy. *Nature* **2020**, *585*, 464−469.
(201) Liberta, F.; Rennegarbe, M.; Rösler, R.; Bijzet, J.; Wiese, S.; Hazenberg, B. P. C.; Fändrich, M. Morphological and Primary Structural Consistency of Fibrils from Different AA Patients (Common Variant). *Amyloid* **2019**, *26*, 164−170.
(202) Westermark, G. T.; Sletten, K.; Westermark, P. Massive Vascular AA-Amyloidosis: A Histologically and Biochemically Distinctive Subtype of Reactive Systemic Amyloidosis. *Scand. J. Immunol.* **1989**, *30*, 605−613.
(203) Bergström, J.; Gustavsson, Å.; Hellman, U.; Sletten, K.; Murphy, C. L.; Weiss, D. T.; Solomon, A.; Olofsson, B.-O.; Westermark, P. Amyloid Deposits in Transthyretin-Derived Amyloidosis: Cleaved Transthyretin Is Associated with Distinct Amyloid Morphology. *J. Pathol.* **2005**, *206*, 224−232.
(204) Raimondi, S.; Mangione, P. P.; Verona, G.; Canetti, D.; Nocerino, P.; Marchese, L.; Piccarducci, R.; Mondani, V.; Faravelli, G.; Taylor, G. W.; et al. Comparative Study of the Stabilities of Synthetic in Vitro and Natural Ex Vivo Transthyretin Amyloid Fibrils. *J. Biol. Chem.* **2020**, *295*, 11379−11387.
(205) Nordstedt, C.; Näslund, J.; Tjernberg, L. O.; Karlström, A. R.; Thyberg, J.; Terenius, L. The Alzheimer a Beta Peptide Develops Protease Resistance in Association with Its Polymerization into Fibrils. *J. Biol. Chem.* **1994**, *269*, 30773−30776.
(206) Aoyagi, A.; Condello, C.; Stöhr, J.; Yue, W.; Rivera, B. M.; Lee, J. C.; Woerman, A. L.; Halliday, G.; van Duinen, S.; Ingelsson, M.; et al. Aβ and Tau Prion-Like Activities Decline with Longevity in the Alzheimer's Disease Human Brain. *Sci. Transl. Med.* **2019**, *11*, No. eaat8462.
(207) Mateju, D.; Franzmann, T. M.; Patel, A.; Kopach, A.; Boczek, E. E.; Maharana, S.; Lee, H. O.; Carra, S.; Hyman, A. A.; Alberti, S. An Aberrant Phase Transition of Stress Granules Triggered by Misfolded Protein and Prevented by Chaperone Function. *EMBO J.* **2017**, *36*, 1669−1687.
(208) Patel, A.; Lee, H. O.; Jawerth, L.; Maharana, S.; Jahnel, M.; Hein, M. Y.; Stoynov, S.; Mahamid, J.; Saha, S.; Franzmann, T. M.; et al. A Liquid-to-Solid Phase Transition of the ALS Protein Fus Accelerated by Disease Mutation. *Cell* **2015**, *162*, 1066−1077.
(209) Zbinden, A.; Pérez-Berlanga, M.; De Rossi, P.; Polymenidou, M. Phase Separation and Neurodegenerative Diseases: A Disturbance in the Force. *Dev. Cell* **2020**, *55*, 45−68.
(210) Jawerth, L.; Fischer-Friedrich, E.; Saha, S.; Wang, J.; Franzmann, T.; Zhang, X.; Sachweh, J.; Ruer, M.; Ijavi, M.; Saha, S.; et al. Protein Condensates as Aging Maxwell Fluids. *Science* **2020**, *370*, 1317−1323.
(211) Mathieu, C.; Pappu, R. V.; Taylor, J. P. Beyond Aggregation: Pathological Phase Transitions in Neurodegenerative Disease. *Science* **2020**, *370*, 56−60.
(212) Namba, Y.; Tomonaga, M.; Kawasaki, H.; Otomo, E.; Ikeda, K. Apolipoprotein E Immunoreactivity in Cerebral Amyloid Deposits and Neurofibrillary Tangles in Alzheimer's Disease and Kuru Plaque Amyloid in Creutzfeldt-Jakob Disease. *Brain Res.* **1991**, *541*, 163−166.
(213) Bellotti, V.; Chiti, F. Amyloidogenesis in Its Biological Environment: Challenging a Fundamental Issue in Protein Misfolding Diseases. *Curr. Opin. Struct. Biol.* **2008**, *18*, 771−779.
(214) Lovell, M. A.; Robertson, J. D.; Teesdale, W. J.; Campbell, J. L.; Markesbery, W. R. Copper, Iron and Zinc in Alzheimer's Disease Senile Plaques. *J. Neurol. Sci.* **1998**, *158*, 47−52.
(215) Ancsin, J. B. Amyloidogenesis: Historical and Modern Observations Point to Heparan Sulfate Proteoglycans as a Major Culprit. *Amyloid* **2003**, *10*, 67−79.
(216) Kollmer, M.; Meinhardt, K.; Haupt, C.; Liberta, F.; Wulff, M.; Linder, J.; Handl, L.; Heinrich, L.; Loos, C.; Schmidt, M.; et al. Electron Tomography Reveals the Fibril Structure and Lipid Interactions in Amyloid Deposits. *Proc. Natl. Acad. Sci. U. S. A.* **2016**, *113*, 5604−5609.
(217) Owen, M. C.; Gnutt, D.; Gao, M.; Wärmländer, S.; Jarvet, J.; Gräslund, A.; Winter, R.; Ebbinghaus, S.; Strodel, B. Effects of in Vivo Conditions on Amyloid Aggregation. *Chem. Soc. Rev.* **2019**, *48*, 3946−3996.
(218) Fichou, Y.; Lin, Y.; Rauch, J. N.; Vigers, M.; Zeng, Z.; Srivastava, M.; Keller, T. J.; Freed, J. H.; Kosik, K. S.; Han, S. Cofactors Are Essential Constituents of Stable and Seeding-Active Tau Fibrils. *Proc. Natl. Acad. Sci. U. S. A.* **2018**, *115*, 13234−13239.
(219) Fichou, Y.; Oberholtzer, Z. R.; Ngo, H.; Cheng, C.-Y.; Keller, T. J.; Eschmann, N. A.; Han, S. Tau-Cofactor Complexes as Building Blocks of Tau Fibrils. *Front. Neurosci.* **2019**, *13*, 1339−1339.
(220) Auzmendi-Iriarte, J.; Matheu, A. Impact of Chaperone-Mediated Autophagy in Brain Aging: Neurodegenerative Diseases and Glioblastoma. *Front. Aging Neurosci.* **2021**, *12*, 630743.
(221) Fatima, K.; Naqvi, F.; Younas, H. A Review: Molecular Chaperone-Mediated Folding, Unfolding and Disaggregation of Expressed Recombinant Proteins. *Cell Biochem. Biophys.* **2021**, *79*, 153−174.
(222) Mays, C. E.; Armijo, E.; Morales, R.; Kramm, C.; Flores, A.; Tiwari, A.; Bian, J.; Telling, G. C.; Pandita, T. K.; Hunt, C. R.; et al. Prion Disease Is Accelerated in Mice Lacking Stress-Induced Heat Shock Protein 70 (Hsp70). *J. Biol. Chem.* **2019**, *294*, 13619−13628.
(223) Bi, M.; Du, X.; Jiao, Q.; Chen, X.; Jiang, H. Expanding the Role of Proteasome Homeostasis in Parkinson's Disease: Beyond Protein Breakdown. *Cell Death Dis.* **2021**, *12*, 154.
(224) Milardi, D.; Gazit, E.; Radford, S. E.; Xu, Y.; Gallardo, R. U.; Caflisch, A.; Westermark, G. T.; Westermark, P.; Rosa, C.; Ramamoorthy, A. Proteostasis of Islet Amyloid Polypeptide: A Molecular Perspective of Risk Factors and Protective Strategies for Type Ii Diabetes. *Chem. Rev.* **2021**, *121*, 1845−1893.
(225) Yang, Y.; Klionsky, D. J. Autophagy and Disease: Unanswered Questions. *Cell Death Differ.* **2020**, *27*, 858−871.
(226) Mallucci, G. R.; Klenerman, D.; Rubinsztein, D. C. Developing Therapies for Neurodegenerative Disorders: Insights from Protein Aggregation and Cellular Stress Responses. *Annu. Rev. Cell Dev. Biol.* **2020**, *36*, 165−189.
(227) Yorimitsu, T.; Klionsky, D. J. Autophagy: Molecular Machinery for Self-Eating. *Cell Death Differ.* **2005**, *12*, 1542−1552.
(228) Mizushima, N. Autophagy: Process and Function. *Genes Dev.* **2007**, *21*, 2861−2873.
(229) Mizushima, N.; Komatsu, M. Autophagy: Renovation of Cells and Tissues. *Cell* **2011**, *147*, 728−741.
(230) Svenning, S.; Johansen, T. Selective Autophagy. *Essays Biochem.* **2013**, *55*, 79−92.
(231) Weidberg, H.; Shvets, E.; Shpilka, T.; Shimron, F.; Shinder, V.; Elazar, Z. LC3 and GATE-16/GABARAP Subfamilies Are Both Essential yet Act Differently in Autophagosome Biogenesis. *EMBO J.* **2010**, *29*, 1792−1802.
(232) Martens, S.; Fracchiolla, D. Activation and Targeting of Atg8 Protein Lipidation. *Cell Discovery* **2020**, *6*, 23.
(233) Johansen, T.; Lamark, T. Selective Autophagy: Atg8 Family Proteins, Lir Motifs and Cargo Receptors. *J. Mol. Biol.* **2020**, *432*, 80−103.
(234) Dikic, I. Proteasomal and Autophagic Degradation Systems. *Annu. Rev. Biochem.* **2017**, *86*, 193−224.
(235) Finley, K. D. Live Long and Prosper: Neural Protection by Enhanced Macroautophagy or Aggrephagy. *Drug Metab. Rev.* **2011**, *43*, 18−19.

https://doi.org/10.1021/acs.chemrev.1c00196
Chem. Rev. 2021, 121, 8285−8307

(236) Yamamoto, A.; Simonsen, A. The Elimination of Accumulated and Aggregated Proteins: A Role for Aggrephagy in Neurodegeneration. *Neurobiol. Dis.* **2011**, *43*, 17−28.
(237) Sun, D. X.; Wu, R. B.; Li, P. L.; Yu, L. Phase Separation in Regulation of Aggrephagy. *J. Mol. Biol.* **2020**, *432*, 160−169.
(238) Tan, S.; Wong, E. Kinetics of Protein Aggregates Disposal by Aggrephagy. *Methods Enzymol.* **2017**, *588*, 245−281.
(239) Chung, C. G.; Lee, H.; Lee, S. B. Mechanisms of Protein Toxicity in Neurodegenerative Diseases. *Cell. Mol. Life Sci.* **2018**, *75*, 3159−3180.
(240) Cheon, S. Y.; Kim, H.; Rubinsztein, D. C.; Lee, J. E. Autophagy, Cellular Aging and Age-Related Human Diseases. *Exp. Neurobiol.* **2019**, *28*, 643−657.
(241) Malampati, S.; Song, J. X.; Chun-Kit Tong, B.; Nalluri, A.; Yang, C. B.; Wang, Z.; Gopalkrishnashetty Sreenivasmurthy, S.; Zhu, Z.; Liu, J.; Su, C. Targeting Aggrephagy for the Treatment of Alzheimer's Disease. *Cells* **2020**, *9*, 311.
(242) Fujikake, N.; Shin, M.; Shimizu, S. Association between Autophagy and Neurodegenerative Diseases. *Front. Neurosci.* **2018**, *12*, 255.
(243) Mizushima, N. A Brief History of Autophagy from Cell Biology to Physiology and Disease. *Nat. Cell Biol.* **2018**, *20*, 521−527.
(244) Bar-Yosef, T.; Damri, O.; Agam, G. Dual Role of Autophagy in Diseases of the Central Nervous System. *Front. Cell. Neurosci.* **2019**, *13*, 196.
(245) Malik, B. R.; Maddison, D. C.; Smith, G. A.; Peters, O. M. Autophagic and Endo-Lysosomal Dysfunction in Neurodegenerative Disease. *Mol. Brain* **2019**, *12*, 100.
(246) Thellung, S.; Corsaro, A.; Nizzari, M.; Barbieri, F.; Florio, T. Autophagy Activator Drugs: A New Opportunity in Neuroprotection from Misfolded Protein Toxicity. *Int. J. Mol. Sci.* **2019**, *20*, 901.
(247) Mputhia, Z.; Hone, E.; Tripathi, T.; Sargeant, T.; Martins, R.; Bharadwaj, P. Autophagy Modulation as a Treatment of Amyloid Diseases. *Molecules* **2019**, *24*, 3372.
(248) Djajadikerta, A.; Keshri, S.; Pavel, M.; Prestil, R.; Ryan, L.; Rubinsztein, D. C. Autophagy Induction as a Therapeutic Strategy for Neurodegenerative Diseases. *J. Mol. Biol.* **2020**, *432*, 2799−2821.
(249) Scrivo, A.; Bourdenx, M.; Pampliega, O.; Cuervo, A. M. Selective Autophagy as a Potential Therapeutic Target for Neurodegenerative Disorders. *Lancet Neurol.* **2018**, *17*, 802−815.
(250) Buratta, S.; Tancini, B.; Sagini, K.; Delo, F.; Chiaradia, E.; Urbanelli, L.; Emiliani, C. Lysosomal Exocytosis, Exosome Release and Secretory Autophagy: The Autophagic- and Endo-Lysosomal Systems Go Extracellular. *Int. J. Mol. Sci.* **2020**, *21*, 2576.
(251) Chiti, F.; Dobson, C. M. Protein Misfolding, Amyloid Formation, and Human Disease: A Summary of Progress over the Last Decade. *Annu. Rev. Biochem.* **2017**, *86*, 27−68.
(252) Frankel, R.; Törnquist, M.; Meisl, G.; Hansson, O.; Andreasson, U.; Zetterberg, H.; Blennow, K.; Frohm, B.; Cedervall, T.; Knowles, T. P. J.; et al. Autocatalytic Amplification of Alzheimer-Associated Aβ42 Peptide Aggregation in Human Cerebrospinal Fluid. *Commun. Biol.* **2019**, *2*, 365.
(253) Lauren, J.; Gimbel, D. A.; Nygaard, H. B.; Gilbert, J. W.; Strittmatter, S. M. Cellular Prion Protein Mediates Impairment of Synaptic Plasticity by Amyloid-β Oligomers. *Nature* **2009**, *457*, 1128−1132.
(254) Zou, W.-Q.; Xiao, X.; Yuan, J.; Puoti, G.; Fujioka, H.; Wang, X.; Richardson, S.; Zhou, X.; Zou, R.; Li, S.; et al. Amyloid-β42 Interacts Mainly with Insoluble Prion Protein in the Alzheimer Brain. *J. Biol. Chem.* **2011**, *286*, 15095−15105.
(255) Bove-Fenderson, E.; Urano, R.; Straub, J. E.; Harris, D. A. Cellular Prion Protein Targets Amyloid-Beta Fibril Ends Via Its C-Terminal Domain to Prevent Elongation. *J. Biol. Chem.* **2017**, *292*, 16858−16871.
(256) Amin, L.; Harris, D. A. Aβ Receptors Specifically Recognize Molecular Features Displayed by Fibril Ends and Neurotoxic Oligomers. *Nat. Commun.* **2021**, *12*, 3451.
(257) Nicoll, A. J.; Panico, S.; Freir, D. B.; Wright, D.; Terry, C.; Risse, E.; Herron, C. E.; O'Malley, T.; Wadsworth, J. D.; Farrow, M. A.; et al. Amyloid-Beta Nanotubes Are Associated with Prion Protein-Dependent Synaptotoxicity. *Nat. Commun.* **2013**, *4*, 2416.
(258) Ferreira, D. G.; Temido-Ferreira, M.; Vicente Miranda, H.; Batalha, V. L.; Coelho, J. E.; Szegö, M.; Marques-Morgado, I.; Vaz, S. H.; Rhee, J. S.; Schmitz, M.; et al. A-Synuclein Interacts with PrP(C) to Induce Cognitive Impairment through mGluR5 and NMDAR2b. *Nat. Neurosci.* **2017**, *20*, 1569−1579.
(259) Ondrejcak, T.; Klyubin, I.; Corbett, G. T.; Fraser, G.; Hong, W.; Mably, A. J.; Gardener, M.; Hammersley, J.; Perkinton, M. S.; Billinton, A.; et al. Cellular Prion Protein Mediates the Disruption of Hippocampal Synaptic Plasticity by Soluble Tau in Vivo. *J. Neurosci.* **2018**, *38*, 10595−10606.
(260) Corbett, G. T.; Wang, Z.; Hong, W.; Colom-Cadena, M.; Rose, J.; Liao, M.; Asfaw, A.; Hall, T. C.; Ding, L.; DeSousa, A.; et al. PrP Is a Central Player in Toxicity Mediated by Soluble Aggregates of Neurodegeneration-Causing Proteins. *Acta Neuropathol.* **2020**, *139*, 503−526.
(261) Resenberger, U. K.; Harmeier, A.; Woerner, A. C.; Goodman, J. L.; Müller, V.; Krishnan, R.; Vabulas, R. M.; Kretzschmar, H. A.; Lindquist, S.; Hartl, F. U.; et al. The Cellular Prion Protein Mediates Neurotoxic Signalling of β-Sheet-Rich Conformers Independent of Prion Replication. *EMBO J.* **2011**, *30*, 2057−2070.
(262) Bate, C.; Williams, A. Amyloid-β-Induced Synapse Damage Is Mediated Via Cross-Linkage of Cellular Prion Proteins. *J. Biol. Chem.* **2011**, *286*, 37955−37963.
(263) Barry, A. E.; Klyubin, I.; McDonald, J. M.; Mably, A. J.; Farrell, M. A.; Scott, M.; Walsh, D. M.; Rowan, M. J. Alzheimer's Disease Brain-Derived Amyloid-β-Mediated Inhibition of LTP in Vivo Is Prevented by Immunotargeting Cellular Prion Protein. *J. Neurosci.* **2011**, *31*, 7259−7263.
(264) Um, J. W.; Nygaard, H. B.; Heiss, J. K.; Kostylev, M. A.; Stagi, M.; Vortmeyer, A.; Wisniewski, T.; Gunther, E. C.; Strittmatter, S. M. Alzheimer Amyloid-β Oligomer Bound to Postsynaptic Prion Protein Activates Fyn to Impair Neurons. *Nat. Neurosci.* **2012**, *15*, 1227−1235.
(265) Um, J. W.; Strittmatter, S. M. Amyloid-β Induced Signaling by Cellular Prion Protein and Fyn Kinase in Alzheimer Disease. *Prion* **2013**, *7*, 37−41.
(266) Balducci, C.; Beeg, M.; Stravalaci, M.; Bastone, A.; Sclip, A.; Biasini, E.; Tapella, L.; Colombo, L.; Manzoni, C.; Borsello, T.; et al. Synthetic Amyloid-β Oligomers Impair Long-Term Memory Independently of Cellular Prion Protein. *Proc. Natl. Acad. Sci. U. S. A.* **2010**, *107*, 2295−2300.
(267) Calella, A. M.; Farinelli, M.; Nuvolone, M.; Mirante, O.; Moos, R.; Falsig, J.; Mansuy, I. M.; Aguzzi, A. Prion Protein and Aβ-Related Synaptic Toxicity Impairment. *EMBO Mol. Med.* **2010**, *2*, 306−314.
(268) Kessels, H. W.; Nguyen, L. N.; Nabavi, S.; Malinow, R. The Prion Protein as a Receptor for Amyloid-β. *Nature* **2010**, *466*, E3−E4.
(269) Cissé, M.; Sanchez, P. E.; Kim, D. H.; Ho, K.; Yu, G.-Q.; Mucke, L. Ablation of Cellular Prion Protein Does Not Ameliorate Abnormal Neural Network Activity or Cognitive Dysfunction in the J20 Line of Human Amyloid Precursor Protein Transgenic Mice. *J. Neurosci.* **2011**, *31*, 10427−10431.
(270) Nieznanski, K.; Choi, J.-K.; Chen, S.; Surewicz, K.; Surewicz, W. K. Soluble Prion Protein Inhibits Amyloid-β (Aβ) Fibrillization and Toxicity. *J. Biol. Chem.* **2012**, *287*, 33104−33108.
(271) Mohammadi, B.; Linsenmeier, L.; Shafiq, M.; Puig, B.; Galliciotti, G.; Giudici, C.; Willem, M.; Eden, T.; Koch-Nolte, F.; Lin, Y.-H.; et al. Transgenic Overexpression of the Disordered Prion Protein N1 Fragment in Mice Does Not Protect against Neurodegenerative Diseases Due to Impaired ER Translocation. *Mol. Neurobiol.* **2020**, *57*, 2812−2829.
(272) Guillot-Sestier, M.-V.; Sunyach, C.; Ferreira, S. T.; Marzolo, M.-P.; Bauer, C.; Thevenet, A.; Checler, F. A-Secretase-Derived Fragment of Cellular Prion, N1, Protects against Monomeric and Oligomeric Amyloid β (Aβ)-Associated Cell Death. *J. Biol. Chem.* **2012**, *287*, 5021−5032.

https://doi.org/10.1021/acs.chemrev.1c00196
Chem. Rev. 2021, 121, 8285−8307

(273) Bove-Fenderson, E.; Urano, R.; Straub, J. E.; Harris, D. A. Cellular Prion Protein Targets Amyloid-β Fibril Ends Via Its C-Terminal Domain to Prevent Elongation. *J. Biol. Chem.* **2017**, *292*, 16858−16871.
(274) Takahashi, R. H.; Tobiume, M.; Sato, Y.; Sata, T.; Gouras, G. K.; Takahashi, H. Accumulation of Cellular Prion Protein within Dystrophic Neurites of Amyloid Plaques in the Alzheimer's Disease Brain. *Neuropathology* **2011**, *31*, 208−214.
(275) Takahashi, R. H.; Yokotsuka, M.; Tobiume, M.; Sato, Y.; Hasegawa, H.; Nagao, T.; Gouras, G. K. Accumulation of Cellular Prion Protein within β-Amyloid Oligomer Plaques in Aged Human Brains. *Brain Pathol.* **2021**, DOI: 10.1111/bpa.12941.
(276) Lewcock, J. W.; Schlepckow, K.; Di Paolo, G.; Tahirovic, S.; Monroe, K. M.; Haass, C. Emerging Microglia Biology Defines Novel Therapeutic Approaches for Alzheimer's Disease. *Neuron* **2020**, *108*, 801−821.
(277) Kober, D. L.; Alexander-Brett, J. M.; Karch, C. M.; Cruchaga, C.; Colonna, M.; Holtzman, M. J.; Brett, T. J. Neurodegenerative Disease Mutations in TREM2 Reveal a Functional Surface and Distinct Loss-of-Function Mechanisms. *eLife* **2016**, *5*, e20391.
(278) Yuan, C.; Aierken, A.; Xie, Z.; Li, N.; Zhao, J.; Qing, H. The Age-Related Microglial Transformation in Alzheimer's Disease Pathogenesis. *Neurobiol. Aging* **2020**, *92*, 82−91.
(279) Kober, D. L.; Stuchell-Brereton, M. D.; Kluender, C. E.; Dean, H. B.; Strickland, M. R.; Steinberg, D. F.; Nelson, S. S.; Baban, B.; Holtzman, D. M.; Frieden, C.; et al. Functional Insights from Biophysical Study of TREM2 Interactions with ApoE and Aβ(1−42). *Alzheimer's Dementia* **2021**, *17*, 475−488.
(280) Cauley, J. A.; Eichner, J. E.; Ilyas Kamboh, M.; Ferrell, R. E.; Kuller, L. H. Apo E Allele Frequencies in Younger (Age 42−50) Vs Older (Age 65−90) Women. *Genet. Epidemiol.* **1993**, *10*, 27−34.
(281) Li, Z.; Shue, F.; Zhao, N.; Shinohara, M.; Bu, G. ApoE2: Protective Mechanism and Therapeutic Implications for Alzheimer's Disease. *Mol. Neurodegener.* **2020**, *15*, 63.
(282) Serrano-Pozo, A.; Das, S.; Hyman, B. T. Apoe and Alzheimer's Disease: Advances in Genetics, Pathophysiology, and Therapeutic Approaches. *Lancet Neurol.* **2021**, *20*, 68−80.
(283) Reyes, J. F.; Ekmark-Lewen, S.; Perdiki, M.; Klingstedt, T.; Hoffmann, A.; Wiechec, E.; Nilsson, P.; Nilsson, K. P. R.; Alafuzoff, I.; Ingelsson, M.; et al. Accumulation of Alpha-Synuclein within the Liver, Potential Role in the Clearance of Brain Pathology Associated with Parkinson's Disease. *Acta Neuropathol. Commun.* **2021**, *9*, 46.

https://doi.org/10.1021/acs.chemrev.1c00196
Chem. Rev. 2021, 121, 8285−8307